PARTITIONED TIMESTEPPING FOR A PARABOLIC TWO DOMAIN PROBLEM

JEFFREY M. CONNORS[*], JASON S. HOWELL[†], AND WILLIAM J. LAYTON[‡]

Abstract. There have been many numerical simulations but few analytical results of stability and accuracy of algorithms for computational modeling of fluid-fluid and fluid-structure interaction problems, where two domains corresponding to different fluids (ocean-atmosphere) or a fluid and deformable solid (blood flow) are separated by an interface. As a simplified model of the first examples, this report considers two heat equations in $\Omega_1, \Omega_2 \subset \mathbb{R}^2$ adjoined by an interface $I = \Omega_1 \cap \Omega_2 \subset \mathbb{R}$. The heat equations are coupled by a condition that allows energy to pass back and forth across the interface I while preserving the total global energy of the monolithic, coupled problem. To compute approximate solutions to the above problem only using subdomain solvers, two first order in time, fully discrete methods are presented. The methods consist of an implicit-explicit (IMEX) approach, in which the action across I is lagged and a partitioned method based on passing interface values back and forth across I. Stability and convergence results are derived for both schemes. Numerical experiments that support the theoretical results are presented.

Key words. fluid-structure interaction, fluid-fluid interaction, ocean-atmosphere, implicit-explicit method.

1. Introduction. There are many problems in which different physical models, different parameter regimes or different solution behaviors are coupled across interfaces. Such problems also arise when legacy codes, highly optimized for particular processes, are considered the benchmark for solving the individual subproblems. One approach to coupled problems is monolithic solution methods. In these the globally coupled problem is assembled at each time step and then solved by iterative methods (with uncoupling in preconditioning and residual calculations). With very large problems or when using legacy codes, partitioned time marching algorithms are preferred. In these the subdomain solvers are used as a black box; each time step involves passing information across the interface followed by solving the individual subproblems independently. Typical applications in which partitioned time stepping approach is highly desirable include atmosphere-ocean coupling and fluid-solid interaction problems, for example, see [7, 8, 10]. In Section 1.2, a motivating atmosphere–ocean coupling problem is described, and a simplified model that is the focus of this work is presented in Section 1.1.

1.1. A Model Problem. In this work, a simplified model of diffusion through two adjacent materials which are coupled across their shared interface I through a jump condition is considered. This problem captures some of the time-stepping difficulties of the ocean-atmosphere problem described in 1.2. The domain consists of two subdomains Ω_1 and Ω_2 coupled across an interface I (example in Figure 1.1 below). The problem is: *given $\nu_i > 0$, $f_i : [0, T] \to H^1(\Omega_i)$, $u_i(0) \in H^1(\Omega_i)$ and $\kappa \in \mathbb{R}$, find (for $i = 1, 2$) $u_i : \overline{\Omega}_i \times [0, T] \to \mathbb{R}$ satisfying*

$$u_{i,t} - \nu_i \Delta u_i = f_i, \quad \text{in } \Omega_i, \tag{1.1}$$

$$-\nu_i \nabla u_i \cdot \hat{n}_i = \kappa(u_i - u_j), \quad \text{on } I, \ i, j = 1, 2, \ i \neq j, \tag{1.2}$$

$$u_i(x, 0) = u_i^0(x), \quad \text{in } \Omega_i, \tag{1.3}$$

$$u_i = g_i, \quad \text{on } \Gamma_i = \partial \Omega_i \setminus I. \tag{1.4}$$

Let

$$X_i := \{v_i \in H^1(\Omega_i) : v_i = 0 \text{ on } \Gamma_i\}.$$

For $u_i \in X_i$ we denote $\mathbf{u} = (u_1, u_2)$ and $X := \{\mathbf{v} = (v_1, v_2) : v_i \in H^1(\Omega_i) : v_i = 0 \text{ on } \Gamma_i, i = 1, 2\}$. A natural subdomain variational formulation for (1.1)-(1.4), obtained by multiplying (1.1) by v_i,

integrating and applying the divergence theorem, is to find (for $i, j = 1, 2, i \neq j$) $u_i : [0, T] \to X_i$ satisfying

$$(u_{i,t}, v_i)_{\Omega_i} + (\nu_i \nabla u_i, \nabla v_i)_{\Omega_i} + \int_I \kappa(u_i - u_j) v_i ds = (f_i, v_i)_{\Omega_i}, \text{ for all } v_i \in X_i. \qquad (1.5)$$

The natural monolithic variational formulation for (1.1)-(1.4) is found by summing (1.5) over $i, j = 1, 2$ and $i \neq j$ and is to find $\mathbf{u} : [0, T] \to X$ satisfying

$$(\mathbf{u}_t, \mathbf{v}) + (\nu \nabla \mathbf{u}, \nabla \mathbf{v}) + \int_I \kappa[\mathbf{u}][\mathbf{v}] ds = (f, \mathbf{v}), \forall v \in X, \qquad (1.6)$$

where $[\cdot]$ denotes the jump of the indicated quantity across the interface I, $(\cdot, \cdot)$ is the $L^2(\Omega_1 \cup \Omega_2)$ inner product and $\nu = \nu_i$ and $f = f_i$ in Ω_i.

Comparing (1.6) and (1.5) we see that *the monolithic, globally coupled problem (1.6) has a monolithic, global energy that is exactly conserved, (in the appropriate sense),* (set $\mathbf{v} = \mathbf{u}$ in (1.6)). *The subdomain sub-problems* (1.5) *do not posses a subdomain energy which behaves similarly due to energy transfer back and forth across the interface I.*

Related domain decomposition methods have been developed for splitting a single heat equation across an interface selected for computational convenience. Dawson and Du [11] analyzed an overlapping method requiring a minimum subdomain overlap for a given mesh width. A weak formulation is defined on the overlapping strip, and the complementary areas of the domain are discretized separately with a procedure to estimate the interface data. Blum, Lisky and Rannacher [5] study uncoupling strategies based on updating data on artificial boundaries of overlapping subdomains via an explicit formula, then solving the problem separately on each subdomain and defining the updated global approximation via an averaging process. Another approach is treating the interface data as a Lagrange multiplier. For an elliptic problem with similarities to (1.1)-(1.4), Burman and Hansbo [9] showed the addition of a penalty term on the interface in a mixed finite element Lagrangian formulation provides a stable, decoupled method with error control.

In this report, two first-order in time, non-overlapping uncoupling methods for (1.1)-(1.4) are presented: a partitioned method, and an implicit-explicit (IMEX) partitioned method. These two are compared to the standard monolithic, coupled implicit method. The main difference between the methods is the manner in which the interface term in (1.5) is advanced in time to give one step black box decoupling of the subdomain problems in Ω_1 and Ω_2.

1.2. A Motivating Problem: Atmosphere-Ocean coupling. Models of atmosphere-ocean interactions often involve many physical processes across multiple space and time scales. An essential feature is the interaction of the flows across an interface I. Three-dimensional, highly optimized codes for each sub-problem's physics and complex physical models make it highly desirable to be able to solve alternately atmosphere and ocean sub-problems by passing information across I. To simplify the problem to that core difficulty, consider advancing the coupled flow of one fluid across I with fluid on the other side of I. Let, as a first step, the interface to be approximated by a rigid lid. Let Ω_1, Ω_2 be the two domains sharing the interface I as a segment of their boundary, as in Figure 1.1. Let n_i, τ_i be the tangent and normal vectors of Ω_i on the interface I, respectively. This leads to the problem for the velocity u_i, pressure p_i and stress Π_i

$$u_{i,t} + u_i \cdot \nabla u_i - \nu_i \Delta u_i + \nabla p_i = f_i, \nabla \cdot u_i = 0 \text{ in } \Omega_i, \qquad (1.7)$$
$$u_i \cdot n_i = 0 \text{ on } I,$$
$$n_i \cdot \Pi_i \cdot \tau_i = \kappa |u_i - u_j| (u_i - u_j), i, j = 1, 2, i \neq j, \text{ on } I \qquad (1.8)$$

with suitable initial conditions and lateral boundary conditions on $\partial\Omega_i \setminus I$, $i = 1, 2$, and $\kappa \in \mathbb{R}$. The key difficulty, like (1.5),(1.6), is that, while the coupled, monolithic, kinetic energy is conserved, the kinetic energy in each subdomain can fluctuate due to energy transport back and forth across the interface I. Incorrect partitioning of the two subdomains can input nonphysical energy into the calculation.
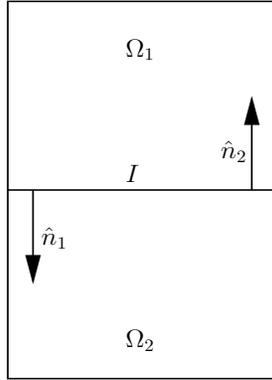
FIG. 1.1. *Example subdomains, coupled across an interface I.*

One approach to such problems is to assemble the monolithic, coupled problem at each step. If the coupled problem is solved by preconditioned iterative methods, uncoupling can occur in the residual calculation and in the preconditioning step. See Bresch and Koko [7] for interesting results. Results are also available for decoupling the fluid-fluid problem using spectral methods, commonly employed in solving fluid problems with periodic boundary conditions (see [4, 17]). There are also problems where, e.g., highly optimized physical parameterizations of each subproblem are built into the subdomain codes. In such problems, the subdomain solvers are best viewed as black boxes when designing the timestepping methods, as the view studied herein.

The remainder of this work is organized as follows: in Section 2, notation and mathematical time-stepping algorithms are described: an IMEX method which partitions the problem by lagging all the interface terms and a partitioned method based on passing interface values across I at each timestep. Results regarding the stability and accuracy of the two partitioned algorithms are presented in Section 3. Convergence results for these methods are presented in Section 4. In Section 5, numerical experiments that support the theoretical results and investigate computational issues are given.

2. Notation and Preliminaries. This section presents the two schemes for (1.1)-(1.4), and provides the necessary definitions and lemmas for their stability and convergence analysis. For $D \subset \Omega$, the Sobolev space $H^k(D) = W^{k,2}(D)$ is equipped with the usual norm $\|\cdot\|_{H^k(D)}$, and semi-norm $|\cdot|_{H^k(D)}$, for $1 \leq k < \infty$, e.g. Adams [1]. The L^2 norm is denoted by $\|\cdot\|_D$. For functions $v(x,t)$ defined for almost every $t \in (0,T)$ on a function space $V(D)$, we define the norms $(1 \leq p \leq \infty)$

$$\|v\|_{L^\infty(0,T;V)} = \operatorname*{ess\,sup}_{0<t<T} \|v(\cdot,t)\|_V \quad \text{and} \quad \|v\|_{L^p(0,T;V)} = \left(\int_0^T \|v\|_V^p \, dt \right)^{1/p} .$$

The dual space of the Banach space V is denoted V'.

Let the domain $\Omega \subset \mathbb{R}^d$ (typically $d = 2, 3$) have convex, polygonal subdomains Ω_i for $i = 1, 2$ with $\partial\Omega_1 \cap \partial\Omega_2 = \Omega_1 \cap \Omega_2 = I$. Let Γ_i denote the portion of $\partial\Omega_i$ that is not on I, i.e. $\Gamma_i = \partial\Omega_i \setminus I$. For $i = 1, 2$, let $X_i = \{v \in H^1(\Omega_i) \mid v|_{\Gamma_i} = g_i\}$, let $(\cdot,\cdot)_{\Omega_i}$ denote the standard L^2 inner product on Ω_i, and let $(\cdot,\cdot)_{X_i}$ denote the standard H^1 inner product on Ω_i. Define $X = X_1 \times X_2$ and $L^2(\Omega) = L^2(\Omega_1) \times L^2(\Omega_2)$ for $\mathbf{u}, \mathbf{v} \in X$ with $\mathbf{u} = [u_1, u_2]^T$ and $\mathbf{v} = [v_1, v_2]^T$, define the L^2 inner product

$$(\mathbf{u}, \mathbf{v}) = \sum_{i=1,2} \int_{\Omega_i} u_i v_i \, dx \, ,$$

and H^1 inner product

$$(\mathbf{u}, \mathbf{v})_X = \sum_{i=1,2} \left(\int_{\Omega_i} u_i v_i \, dx + \int_{\Omega_i} \nabla u_i \cdot \nabla v_i \, dx \right) ,$$

3

and the induced norms $\|\mathbf{v}\| = (\mathbf{v}, \mathbf{v})^{1/2}$ and $\|\mathbf{v}\|_X = (\mathbf{v}, \mathbf{v})_X^{1/2}$, respectively. The case where $g_i = 0, i = 1, 2$ will be considered here, and can be easily extended to the case of nonhomogeneous Dirichlet conditions on $\partial\Omega_i \setminus I$.

LEMMA 2.1. $(X, \|\cdot\|_X)$ is a Hilbert space.

Proof. The choice of boundary conditions for X_1 and X_2 will ensure $X_i \subset H^1(\Omega_i)$, $i = 1, 2$ are closed subspaces. Hence by the definitions of $(\cdot, \cdot)_X$ and $\|\cdot\|_X$, $(X, \|\cdot\|_X)$ is a Hilbert space. $\square$

2.1. Discrete Formulation. Let $\mathcal{T}_i$ be a triangulation of Ω_i and $\mathcal{T}_h = \mathcal{T}_1 \cup \mathcal{T}_2$. Take $X_{i,h} \subset X_i$ to be conforming finite element spaces for $i = 1, 2$, and define $X_h = X_{1,h} \times X_{2,h} \subset X$. It follows that $X_h \subset X$ is a Hilbert space with corresponding inner product and induced norm. For $\mathbf{u} \in X$, define the operators $A, B : X \to (X)'$ via the Riesz Representation Theorem as

$$\big(A\mathbf{u}, \mathbf{v}\big) = \sum_{i=1,2} \nu_i \int_{\Omega_i} \nabla u_i : \nabla v_i \, dx, \quad \forall \mathbf{v} \in X \text{ and} \tag{2.1}$$

$$\big(B\mathbf{u}, \mathbf{v}\big) = \kappa \int_I [\mathbf{u}] \, [\mathbf{v}] \, ds, \ \forall \mathbf{v} \in X . \tag{2.2}$$

The discrete operators $A_h, B_h : X_h \to (X_h)' = X_h$ are defined analogously by restricting (2.1) and (2.2) to $\mathbf{v}_h \in X_h$. With this notation the coupled problem can be written

$$\frac{\partial \mathbf{u}}{\partial t} + A\mathbf{u} + B\mathbf{u} = \mathbf{f}, \ \mathbf{u}(x, 0) = \mathbf{u}_0. \tag{2.3}$$

For $t_k \in [0, T]$, $\mathbf{u}^k$ will denote the discrete approximation to $\mathbf{u}(t_k)$.

2.1.1. Fully Implicit Scheme. We use the fully implicit coupled scheme as a point of comparison with the two partitioned ones we study. The monolithic, globally coupled Backward Euler in time, FEM in space method is as follows. Given $u_1^n \in X_1^h, u_2^n \in X_2^h$ solve globally (for $i, j = 1, 2, i \neq j$) for $u_1^{n+1} \in X_1^h, u_2^{n+1} \in X_2^h$ satisfying

$$\left(\frac{u_i^{n+1} - u_i^n}{\triangle t}, v_i\right)_{\Omega_i} + (\nu_i \nabla u_i^{n+1}, \nabla v_i)_{\Omega_i} + \int_I \kappa(u_i^{n+1} - u_j^{n+1}) v_i ds = (f_i^{n+1}, v_i)_{\Omega_i}, \ \forall v_i \in X_i^h. \tag{2.4}$$

This standard first-order implicit scheme can be written as follows.

ALGORITHM 2.1 (Implicit Scheme). *Let $\triangle t > 0$, $\mathbf{f} \in L^2(\Omega)$. For each $M \in \mathbb{N}, M \leq \frac{T}{\triangle t}$, given $\mathbf{u}^n \in X_h$, $n = 0, 1, 2, \cdots, M - 1$, find $\mathbf{u}^{n+1} \in X_h$ satisfying*

$$\frac{\mathbf{u}^{n+1} - \mathbf{u}^n}{\triangle t} + A_h \mathbf{u}^{n+1} + B_h \mathbf{u}^{n+1} = \mathbf{f}(t^{n+1}) . \tag{2.5}$$

The monolithic implicit scheme (2.5) is unconditionally stable. To see this, set $\mathbf{u} = (u_1, u_2), \nu = (\nu_1, \nu_2)$ in $\Omega = (\Omega_1, \Omega_2)$. If (2.4) is summed it is obvious that the true solution's energy is bounded (set $\mathbf{v} = \mathbf{u}$ below). Indeed, $\mathbf{u}$ satisfies:

$$\left(\frac{\mathbf{u}_i^{n+1} - \mathbf{u}_i^n}{\triangle t}, \mathbf{v}\right) + (\nu \nabla \mathbf{u}^{n+1}, \nabla \mathbf{v}) + \int_I \kappa[\mathbf{u}^{n+1}][\mathbf{v}] ds = (f, \mathbf{v}), \tag{2.6}$$

and setting $\mathbf{v} = \mathbf{u}^{n+1}$ one verifies stability of the monolithic method.

2.1.2. The Implicit-Explicit Partitioned Scheme. The calculations in (2.4),(2.5),(2.6) uncouple into subdomain solves if the B_h term in (2.5) (the interface term) is lagged. This is equivalent to using an IMEX scheme in (2.3) and is a standard partitioned time stepping method. Passing u_j^n across I, this reads: given $u_1^n \in X_1^h, u_2^n \in X_2^h$ (passed across I as known data) solve on each subdomain (for $i, j = 1, 2, i \neq j$) for $u_1^{n+1} \in X_1^h, u_2^{n+1} \in X_2^h$

$$\left(\frac{u_i^{n+1} - u_i^n}{\triangle t}, v_i\right)_{\Omega_i} + (\nu_i \nabla u_i^{n+1}, \nabla v_i)_{\Omega_i} + \int_I \kappa(u_i^n - u_j^n) v_i ds = (f_i, v_i)_{\Omega_i}. \tag{2.7}$$

4

IMEX schemes have been commonly employed in a variety of applications, including incompressible fluid calculations, [2, 3, 14]. If the operators A_h and B_h defined above are simultaneously diagonalizable, one may rewrite the discrete equations using an eigenbasis common to A_h and B_h and derive a stability condition like

$$|1 - \Delta t \mu_j| \leq |1 + \Delta t \lambda_j|, \ j = 1, 2, \cdots, N,$$

where N is the dimension of X_h and A_h and B_h have eigenvalues $\{\lambda_j\}_{j=1}^N$ and $\{\mu_j\}_{j=1}^N$, respectively. Using the fact that the maximum eigenvalue of B_h is order h^{-1} when X_h satisfies an inverse inequality, stability is then guaranteed under a timestep restriction $\Delta t \leq C h$. In the present context, A_h and B_h are not assumed to commute, and thus eigenmode stability results are not applicable. Some stability results for this (simplest) IMEX method have been proven in [2, 14].

In fluid-structure interaction (FSI) problems the analogous time stepping method has been observed to exhibit exponential energy growth, [10]. Burman and Fernández [8] have shown for a simplified FSI problem that a penalty term added to the interface operator provides stabilization, and first-order accuracy in time can be recovered using defect correction. In Theorem 4.2 we show that the partitioned method (2.7) is unconditionally stable (in the discretization parameters) for the global problem (under a condition on the coupling coefficient κ and viscosities ν_i).

ALGORITHM 2.2 (First-order IMEX Scheme). *Let $\Delta t > 0$, $\mathbf{f} \in L^2(\Omega)$. For each $M \in \mathbb{N}, M \leq \frac{T}{\Delta t}$, given $\mathbf{u}^n \in X_h$, $n = 0, 1, 2, \cdots, M-1$, find $\mathbf{u}^{n+1} \in X_h$ satisfying*

$$\frac{\mathbf{u}^{n+1} - \mathbf{u}^n}{\Delta t} + A_h \mathbf{u}^{n+1} + B_h \mathbf{u}^n = \mathbf{f}(t^{n+1}), \tag{2.8}$$

or, in variational form,

$$\left(\frac{\mathbf{u}^{n+1} - \mathbf{u}^n}{\Delta t}, \mathbf{v} \right) + \left(A_h \mathbf{u}^{n+1}, \mathbf{v} \right) + \left(B_h \mathbf{u}^n, \mathbf{v} \right) = \left(\mathbf{f}(t^{n+1}), \mathbf{v} \right), \ \forall \mathbf{v} \in X_h. \tag{2.9}$$

Adapting a stability result in Section 3, it shall be shown in Theorem 4.1 that this method is stable provided

$$\Delta t \leq C \min\{\nu_1, \nu_2\} \kappa^{-2}.$$

2.1.3. A Data-Passing Partitioned Scheme. The second partitioned method we study decouples by solving the problems on Ω_i with interface data for $u_j, i \neq j$ coming from the previous time step. Requiring each linear solve to incorporate the interface operator sacrifices flexibility in implementation in exchange for a more accurate and stable scheme (Sections 3,4), while still admitting an easy parallelization. This method is: given $u_1^n \in X_1^h, u_2^n \in X_2^h$ solve on each subdomain (for $i, j = 1, 2, i \neq j$) for $u_1^{n+1} \in X_1^h, u_2^{n+1} \in X_2^h$

$$\left(\frac{u_i^{n+1} - u_i^n}{\triangle t}, v_i \right)_{\Omega_i} + (\nu_i \nabla u_i^{n+1}, \nabla v_i)_{\Omega_i} + \int_I \kappa(u_i^{n+1} - u_j^n) v_i ds = (f_i, v_i)_{\Omega_i}. \tag{2.10}$$

Summing (2.10) over $i = 1, 2$ gives an equivalent form to (2.10).

ALGORITHM 2.3 (Partitioned Scheme). *Let $\Delta t > 0$, $\mathbf{f} \in L^2(\Omega)$. For each $M \in \mathbb{N}, M \leq \frac{T}{\Delta t}$, given $\mathbf{u}^n \in X_h$, $n = 0, 1, 2, \cdots, M-1$, find $\mathbf{u}^{n+1} \in X_h$ satisfying*

$$\left(\frac{u_i^{n+1} - u_i^n}{\Delta t}, v_i \right) + \nu_i \left(\nabla u_i^{n+1}, \nabla v_i \right) + \kappa \int_I (u_i^{n+1} - u_j^n) v_i \, ds$$
$$= \left(f_i(t^{n+1}), v_i \right), \ i \neq j, \ \forall v_i \in X_{i,h}. \tag{2.11}$$

2.2. Analytical Tools. In this section results that will be utilized in the stability and convergence analysis are presented. It is necessary to work with norms induced by the operators A and B, and relate these norms back to $\|\cdot\|$ and $\|\cdot\|_X$. The next lemma serves to introduce useful norms for the numerical analysis and prove equivalence with the $\|\cdot\|_X$-norm.

LEMMA 2.2. *Let* $\mathbf{v} = (v_1, v_2) \in X$ *and* $\alpha \geq 0$. *The following is a norm on* X:

$$\|\mathbf{v}\|_{A+\alpha I} = \left\{ \sum_{i=1,2} \nu_i \int_{\Omega_i} |\nabla v_i|^2 \, dx + \alpha \sum_{i=1,2} \int_{\Omega_i} |v_i|^2 \, dx \right\}^{1/2}. \tag{2.12}$$

This norm is equivalent to $\|\cdot\|_X$. *For* $\alpha \geq C \kappa^2 \max\{\nu_1^{-1}, \nu_2^{-1}\}$,

$$\kappa \int_I [\mathbf{v}]^2 \, ds \leq \sum_{i=1,2} \nu_i \int_{\Omega_i} |\nabla v_i|^2 \, dx + \alpha \sum_{i=1,2} \int_{\Omega_i} |v_i|^2 \, dx, \text{ and thus}$$

$$\|\mathbf{v}\|_{A+\alpha I - B} = \left\{ \sum_{i=1,2} \nu_i \int_{\Omega_i} |\nabla v_i|^2 \, dx + \alpha \sum_{i=1,2} \int_{\Omega_i} |v_i|^2 \, dx - \kappa \int_I |v_1 - v_2|^2 \, ds \right\}^{1/2}$$

is a norm on X *equivalent to* $\|\cdot\|_X$.

Proof. The first assertion follows from noting the Poincaré–Friedrichs inequality holds on X_1 and X_2 under the boundary conditions, and thus that the norm is derived from an inner product on X. Then equivalence to the norm $\|\cdot\|_X$ is clear. It can also be shown that $\|\mathbf{v}\|_{A+\alpha I - B}$ is derived from an inner product by defining

$$(\mathbf{u}, \mathbf{v})_{A+\alpha I - B} = \sum_{i=1,2} \nu_i \int_{\Omega_i} \nabla u_i : \nabla v_i \, dx + \alpha \sum_{i=1,2} \int_{\Omega_i} u_i \cdot v_i \, dx - \kappa \int_I (u_1 - u_2)(v_1 - v_2) \, ds.$$

Linearity and symmetry are clear. It remains to prove definiteness and equivalence to $\|\cdot\|_A$. Note that

$$\kappa \int_I |v_1 - v_2|^2 \, ds \leq \kappa \left\{ \|v_1\|_{L^2(I)}^2 + 2\|v_1\|_{L^2(I)}\|v_2\|_{L^2(I)} + \|v_2\|_{L^2(I)}^2 \right\}$$

$$\leq 2\kappa \left\{ \|v_1\|_{L^2(I)}^2 + \|v_2\|_{L^2(I)}^2 \right\}$$

$$= 2\kappa \left\{ \|v_1\|_{L^2(\partial\Omega_1)}^2 + \|v_2\|_{L^2(\partial\Omega_2)}^2 \right\}.$$

Application of the trace inequality [6] followed by Young's inequality yields

$$\kappa \int_I |v_1 - v_2|^2 \, ds \leq C(\kappa, \Omega_1, \Omega_2) \left\{ \|v_1\|_{L^2(\Omega_1)}\|\nabla v_1\|_{L^2(\Omega_1)} + \|v_2\|_{L^2(\Omega_2)}\|\nabla v_2\|_{L^2(\Omega_2)} \right\}$$

$$\leq C(\kappa, \Omega_1, \Omega_2) \left\{ \frac{1}{2\gamma_1}\|v_1\|_{L^2(\Omega_1)}^2 + \frac{\gamma_1}{2}\|\nabla v_1\|_{L^2(\Omega_1)}^2 + \frac{1}{2\gamma_2}\|v_2\|_{L^2(\Omega_2)}^2 + \frac{\gamma_2}{2}\|\nabla v_2\|_{L^2(\Omega_2)}^2 \right\}.$$

Choose $\gamma_i = \dfrac{\nu_i}{C(\kappa, \Omega_1, \Omega_2)}$ for $i = 1, 2$ and $\alpha = \dfrac{C(\kappa, \Omega_1, \Omega_2)^2}{2} \max\{\nu_1^{-1}, \nu_2^{-1}\}$. Then

$$\kappa \int_I |v_1 - v_2|^2 \, ds \leq \alpha\|v_1\|_{L^2(\Omega_1)}^2 + \frac{\nu_1}{2}\|\nabla v_1\|_{L^2(\Omega_1)}^2 + \alpha\|v_2\|_{L^2(\Omega_2)}^2 + \frac{\nu_2}{2}\|\nabla v_2\|_{L^2(\Omega_2)}^2$$

$$\Rightarrow \frac{1}{2} \left\{ \nu_1\|\nabla v_1\|_{L^2(\Omega_1)}^2 + \nu_2\|\nabla v_2\|_{L^2(\Omega_2)}^2 \right\}$$

$$\leq \sum_{i=1,2} \nu_i \int_{\Omega_i} |\nabla v_i|^2 \, dx + \alpha \sum_{i=1,2} \int_{\Omega_i} |v_i|^2 \, dx - \kappa \int_I |v_1 - v_2|^2 \, ds$$

$$\Rightarrow \frac{1}{2}\|\mathbf{v}\|_A^2 \leq \|\mathbf{v}\|_{A+\alpha I - B}^2.$$

6

holds for this choice of $\alpha > 0$. This proves $(\mathbf{u}, \mathbf{u})_{A+\alpha I - B} = 0 \Leftrightarrow \mathbf{u} = 0$ for any $\mathbf{u} \in X$, and hence $\|\cdot\|_{A+\alpha I - B}$ is a norm on X. Last, to prove equivalence with $\|\cdot\|_A$, note that

$$\|\mathbf{v}\|_{A+\alpha I - B}^2 \leq \|\mathbf{v}\|_{A+\alpha I}^2 = \sum_{i=1,2} \left\{ \alpha \|v_i\|_{L^2(\Omega_i)}^2 + \nu_i \|\nabla v_i\|_{L^2(\Omega_i)}^2 \right\}$$

$$\leq \left\{ 1 + \alpha \max \left\{ \frac{C_{PF}^2(\Omega_1)}{\nu_1}, \frac{C_{PF}^2(\Omega_2)}{\nu_2} \right\} \right\} \|\mathbf{v}\|_A^2.$$

holds by applying the Poincaré - Friedrichs inequality. $\square$

The following discrete Gronwall lemma from [13] will also be utilized in the subsequent analysis.

LEMMA 2.3. *Let k, M, and $a_\mu, b_\mu, c_\mu, \gamma_\mu$, for integers $\mu > 0$, be nonnegative numbers such that*

$$a_n + k \sum_{\mu=0}^n b_\mu \leq k \sum_{\mu=0}^n \gamma_\mu a_\mu + k \sum_{\mu=0}^n c_\mu + M \text{ for } n \geq 0. \tag{2.13}$$

Suppose that $k\gamma_\mu < 1$, for all μ, and set $\sigma_\mu \equiv (1 - k\gamma_\mu)^{-1}$. Then,

$$a_n + k \sum_{\mu=0}^n b_\mu \leq exp\left(k \sum_{\mu=0}^n \sigma_\mu \gamma_\mu \right) \left\{ k \sum_{\mu=0}^n c_\mu + M \right\} \text{ for } n \geq 0. \tag{2.14}$$

3. Stability. Stability of the approximations in Algorithm 2.2 and Algorithm 2.3 is established here.

LEMMA 3.1. *(IMEX Stability) Let $\mathbf{u}^{n+1} \in X^h$ satisfy (2.9) for each $n \in \left\{ 0, 1, 2, \cdots, \frac{T}{\Delta t} - 1 \right\}$, and $0 < \Delta t < (2\alpha + 1)^{-1}$. Then $\exists C_1, C_2 > 0$ independent of h, Δt such that $\mathbf{u}^{n+1}$ satisfies:*

$$\left\| \mathbf{u}^{n+1} \right\|^2 + \Delta t \sum_{k=0}^{n+1} \|\mathbf{u}^k\|_X^2 \leq C_1(\alpha) e^{C_2(\alpha)T} \left\{ \|\mathbf{u}^0\|^2 + \Delta t \|\mathbf{u}^0\|_X^2 + \Delta t \sum_{k=0}^n \|\mathbf{f}(t^{k+1})\|^2 \right\}.$$

Proof. Choose $\mathbf{v} = \mathbf{u}^{k+1}$ in (2.9). Then it follows:

$$\left(\frac{\mathbf{u}^{k+1} - \mathbf{u}^k}{\Delta t}, \mathbf{u}^{k+1} \right) + \left(A_h \mathbf{u}^{k+1}, \mathbf{u}^{k+1} \right) + \left(C_h \mathbf{u}^k, \mathbf{u}^{k+1} \right) = \left(\mathbf{f}(t^{k+1}), \mathbf{u}^{k+1} \right).$$

Add $\alpha(\mathbf{u}^{k+1}, \mathbf{u}^{k+1})$ to both sides and apply (2.12). Then apply Young's inequality to bound below the term

$$\left(\frac{\mathbf{u}^{k+1} - \mathbf{u}^k}{\Delta t}, \mathbf{u}^{k+1} \right) \geq \frac{1}{2\Delta t} \left(\|\mathbf{u}^{k+1}\|^2 - \|\mathbf{u}^k\|^2 \right),$$

resulting in

$$\frac{1}{2\Delta t} \left(\|\mathbf{u}^{k+1}\|^2 - \|\mathbf{u}^k\|^2 \right) + \|\mathbf{u}^{k+1}\|_{A+\alpha I}^2 + \left(B_h \mathbf{u}^k, \mathbf{u}^{k+1} \right) \leq \left(\mathbf{f}(t^{k+1}), \mathbf{u}^{k+1} \right) + \alpha \|\mathbf{u}^{k+1}\|^2.$$

Now

$$\left(B_h \mathbf{u}^k, \mathbf{u}^{k+1} \right) \geq -\frac{1}{2} \left(B_h \mathbf{u}^{k+1}, \mathbf{u}^{k+1} \right) - \frac{1}{2} \left(B_h \mathbf{u}^k, \mathbf{u}^k \right).$$

Then split the term

$$\|\mathbf{u}^{k+1}\|_{A+\alpha I}^2 = \frac{1}{2} \|\mathbf{u}^{k+1}\|_{A+\alpha I}^2 + \frac{1}{2} \left(\|\mathbf{u}^{k+1}\|_{A+\alpha I}^2 - \|\mathbf{u}^k\|_{A+\alpha I}^2 \right) + \frac{1}{2} \|\mathbf{u}^k\|_{A+\alpha I}^2.$$

These results imply the new estimate

$$\frac{1}{2\Delta t} \left(\|\mathbf{u}^{k+1}\|^2 - \|\mathbf{u}^k\|^2 \right) + \frac{1}{2} \|\mathbf{u}^{k+1}\|_{A+\alpha I - B}^2 + \frac{1}{2} \left(\|\mathbf{u}^{k+1}\|_{A+\alpha I}^2 - \|\mathbf{u}^k\|_{A+\alpha I}^2 \right) + \frac{1}{2} \|\mathbf{u}^k\|_{A+\alpha I - B}^2$$
$$\leq \left(\mathbf{f}(t^{k+1}), \mathbf{u}^{k+1} \right) + \alpha \|\mathbf{u}^{k+1}\|^2.$$

7

Apply Hölder's and Young's inequality on the RHS. Summing over $k = 0, 1, 2, \cdots, n$ yields

$$\frac{1}{2\Delta t}\left(\|\mathbf{u}^{n+1}\|^2 - \|\mathbf{u}^0\|^2\right) + \frac{1}{2}\left(\|\mathbf{u}^{n+1}\|^2_{A+\alpha I} - \|\mathbf{u}^0\|^2_{A+\alpha I}\right)$$
$$+ \frac{1}{2}\sum_{k=0}^n \left\{\|\mathbf{u}^{k+1}\|^2_{A+\alpha I - B} + \|\mathbf{u}^k\|^2_{A+\alpha I - B}\right\}$$
$$\leq \frac{1}{2}\sum_{k=0}^n \|\mathbf{f}(t^{k+1})\|^2 + \frac{2\alpha+1}{2}\sum_{k=0}^n \|\mathbf{u}^{k+1}\|^2.$$

Rearranging terms,

$$\|\mathbf{u}^{n+1}\|^2 + \Delta t\|\mathbf{u}^{n+1}\|^2_{A+\alpha I} + \Delta t \sum_{k=0}^n \left\{\|\mathbf{u}^{k+1}\|^2_{A+\alpha I - B} + \|\mathbf{u}^k\|^2_{A+\alpha I - B}\right\}$$
$$\leq \|\mathbf{u}^0\|^2 + \Delta t\|\mathbf{u}^0\|^2_{A+\alpha I} + \Delta t \sum_{k=0}^n \|\mathbf{f}(t^{k+1})\|^2 + \Delta t(2\alpha+1)\sum_{k=0}^n \|\mathbf{u}^{k+1}\|^2.$$

Taking $\gamma_n \equiv 2\alpha + 1$ in Lemma 2.3, it follows that

$$\|\mathbf{u}^{n+1}\|^2 + \Delta t\|\mathbf{u}^{n+1}\|^2_{A+\alpha I} + \Delta t \sum_{k=0}^n \left\{\|\mathbf{u}^{k+1}\|^2_{A+\alpha I - B} + \|\mathbf{u}^k\|^2_{A+\alpha I - B}\right\}$$
$$\leq e^{C_2(\alpha)T}\left\{\|\mathbf{u}^0\|^2 + \Delta t\|\mathbf{u}^0\|^2_{A+\alpha I} + \Delta t \sum_{k=0}^n \|\mathbf{f}(t^{k+1})\|^2\right\},$$

where $C_2(\alpha) = (2\alpha+1)(1 - \Delta t(2\alpha+1)^{-1})$. Applying Lemma 2.2 and simple inequalities determines $C_1(\alpha)$, and the final result. $\square$

Unlike the IMEX scheme, the data-passing partitioned algorithm is stable when κ is large compared to the dissipation constants ν_1, ν_2.

LEMMA 3.2. *(Data-Passing Partitioned Stability) Let* $\mathbf{u}^{n+1} \in X^h$ *satisfy (2.11) for each* $n \in \left\{0, 1, \cdots, \frac{T}{\Delta t} - 1\right\}$. *Then* $\exists C > 0$ *independent of* $h, \Delta t$ *such that* $\mathbf{u}^{n+1}$ *satisfies:*

$$\left\|\mathbf{u}^{n+1}\right\|^2 + \Delta t\left\|\mathbf{u}^{n+1}\right\|^2_I + \Delta t \sum_{k=0}^{n+1} \|\mathbf{u}^k\|^2_X \leq C\left\{\|\mathbf{u}^0\|^2 + \Delta t\|\mathbf{u}^0\|^2_I + \Delta t \sum_{k=0}^n \|\mathbf{f}(t^{k+1})\|^2\right\}.$$

Proof. Choose $\mathbf{v} = \mathbf{u}^{k+1}$ in (2.11). Then it follows:

$$\left(\frac{u_i^{k+1} - u_i^k}{\Delta t}, u_i^{k+1}\right)_{\Omega_i} + \nu_i\|\nabla u_i^{k+1}\|^2_{\Omega_i} + \kappa\int_I (u_i^{k+1} - u_j^k)u_i^{k+1}\, ds = \left(f_i(t^{k+1}), u_i^{k+1}\right)_{\Omega_i}, \ i \neq j.$$

Rearrange terms and bound the LHS below as in Lemma 3.1,

$$\frac{1}{2\Delta t}\left(\|u_i^{k+1}\|^2_{\Omega_i} - \|u_i^k\|^2_{\Omega_i}\right) + \nu_i\|\nabla u_i^{k+1}\|^2_{\Omega_i} + \kappa\|u_i^{k+1}\|^2_I$$
$$= \left(f_i(t^{k+1}), u_i^{k+1}\right)_{\Omega_i} + \kappa\int_I u_j^k u_i^{k+1}\, ds$$
$$\leq C_{PF}(\Omega_i)\|f_i(t^{k+1})\|_{\Omega_i}\|\nabla u_i^{k+1}\|_{\Omega_i} + \kappa\|u_j^k\|_I\|u_i^{k+1}\|_I.$$

Young's inequality is applied next on the RHS. Summing over $i, j = 1, 2, \ i \neq j$ yields

$$\frac{1}{2\Delta t}\left(\|\mathbf{u}^{k+1}\|^2 - \|\mathbf{u}^k\|^2\right) + \frac{1}{2}\|\mathbf{u}^{k+1}\|^2_A + \frac{\kappa}{2}\left(\|\mathbf{u}^{k+1}\|^2_I - \|\mathbf{u}^k\|^2_I\right)$$
$$\leq C(\nu_1^{-1}, \nu_2^{-1})\|f(t^{k+1})\|^2.$$

8

Multiply through by $2\Delta t$ and sum over $k = 0, 1, \cdots, n$:

$$\|\mathbf{u}^{n+1}\|^2 - \|\mathbf{u}^0\|^2 + \Delta t \sum_{k=0}^{n} \|\mathbf{u}^{k+1}\|_A^2 + \kappa \Delta t \left(\|\mathbf{u}^{n+1}\|_I^2 - \|\mathbf{u}^0\|_I^2 \right)$$

$$\leq C(\nu_1^{-1}, \nu_2^{-1}) \Delta t \sum_{k=0}^{n} \|f(t^{k+1})\|^2.$$

Add the initial data to the right hand side. Then applying Lemma 2.2 and simple inequalities yields the final result.
□

4. Convergence. The necessary theoretical framework is in place to proceed to the convergence analysis for Algorithm 2.2 and Algorithm 2.3. Algorithm 2.1 is unconditionally stable and converges optimally in the same discrete energy norm of Theorem 4.1, the proof of which is straightforward.

THEOREM 4.1. *(Convergence of the IMEX scheme) Let $\mathbf{u}(t; x) \in X$ for all $t \in (0, T)$ solve (1.1)–(1.4), such that $\mathbf{u}_t \in L^2(0, T; X)$ and $\mathbf{u}_{tt} \in L^2(0, T; L^2(\Omega))$. Then $\exists C_1, C_2 > 0$ independent of $h, \Delta t$ such that for any $n \in \{0, 1, 2, \cdots, M - 1 = \frac{T}{\Delta t} - 1\}$ and $0 < \Delta t < (2 + 2\alpha)^{-1}$, the solution $\mathbf{u}^{n+1} \in X_h$ of (2.9) satisfies:*

$$\|\mathbf{u}(t^{n+1}) - \mathbf{u}^{n+1}\|^2 + \Delta t \|\mathbf{u}(t^{n+1}) - \mathbf{u}^{n+1}\|_X^2 + \frac{3\Delta t}{4} \sum_{k=0}^{n} \|\mathbf{u}(t^{k+1}) - \mathbf{u}^{k+1}\|_X^2$$

$$\leq C_1(\alpha) e^{C_2(\alpha) T} \Big\{ \|\mathbf{u}(0) - \mathbf{u}^0\|^2 + \Delta t \|\mathbf{u}(0) - \mathbf{u}^0\|_X^2 + \Delta t^2 \|\mathbf{u}_t\|_{L^2(0,T;X)}^2$$

$$+ \Delta t^2 \|\mathbf{u}_{tt}\|_{L^2(0,T;L^2(\Omega))}^2$$

$$+ \inf_{\mathbf{v}^0 \in X_h} \left\{ \|\mathbf{u}(0) - \mathbf{v}^0\|^2 + \Delta t \|\mathbf{u}(0) - \mathbf{v}^0\|_X^2 \right\} + \inf_{\mathbf{v} \in X_h} \|(\mathbf{u}(0) - \mathbf{v})_t\|^2$$

$$+ T \max_{k=1,2,\cdots,n+1} \inf_{\mathbf{v}^k \in X_h} \|\mathbf{u}(t^k) - \mathbf{v}^k\|_X^2 \Big\}.$$

Proof. Restricting test functions to X_h, subtract (2.9) from (1.6) to get the error equation:

$$\left(\mathbf{u}_t(t^{k+1}) - \frac{\mathbf{u}^{k+1} - \mathbf{u}^k}{\Delta t}, \mathbf{v} \right) + \left(A(\mathbf{u}(t^{k+1}) - \mathbf{u}^{k+1}), \mathbf{v} \right) + \left(B(\mathbf{u}(t^{k+1}) - \mathbf{u}^k), \mathbf{v} \right) = 0.$$

Define $\mathbf{r}^{k+1} = \mathbf{u}_t(t^{k+1}) - \frac{\mathbf{u}(t^{k+1}) - \mathbf{u}(t^k)}{\Delta t}$ and rearrange terms.

$$\left(\mathbf{r}^{k+1}, \mathbf{v} \right) + \left(\frac{\mathbf{u}(t^{k+1}) - \mathbf{u}^{k+1}}{\Delta t} - \frac{\mathbf{u}(t^k) - \mathbf{u}^k}{\Delta t}, \mathbf{v} \right) + \left(A(\mathbf{u}(t^{k+1}) - \mathbf{u}^{k+1}), \mathbf{v} \right)$$

$$+ \left(B(\mathbf{u}(t^{k+1}) - \mathbf{u}^k), \mathbf{v} \right) = 0, \ \forall \mathbf{v} \in X_h. \tag{4.1}$$

Define for each $k = 0, 1, 2, \cdots$ the functions $(\mathbf{u}(t^k) - \mathbf{v}^k) + (\mathbf{v}^k - \mathbf{u}^k) = \boldsymbol{\eta}^k + \boldsymbol{\phi}^k$, where $\mathbf{v}^k \in X_h$ is arbitrary. Then by adding and subtracting $\mathbf{v}^k$ where appropriate, (4.1) may be rewritten as

$$\frac{1}{\Delta t} \left(\boldsymbol{\phi}^{k+1} - \boldsymbol{\phi}^k, \mathbf{v} \right) + \left(A\boldsymbol{\phi}^{k+1}, \mathbf{v} \right) + \left(B(\mathbf{u}(t^{k+1}) - \mathbf{u}^k), \mathbf{v} \right)$$

$$= -\frac{1}{\Delta t} \left(\boldsymbol{\eta}^{k+1} - \boldsymbol{\eta}^k, \mathbf{v} \right) - \left(\mathbf{r}^{k+1}, \mathbf{v} \right) - \left(A\boldsymbol{\eta}^{k+1}, \mathbf{v} \right), \ \forall \mathbf{v} \in X_h. \tag{4.2}$$

To treat the B-term, only first-order accuracy in time need be maintained, so adding and subtracting $B\mathbf{u}(t^k)$, it follows

$$B\mathbf{u}(t^{k+1}) - B\mathbf{u}^k = B(\mathbf{u}(t^{k+1}) - \mathbf{u}(t^k)) + B\boldsymbol{\eta}^k + B\boldsymbol{\phi}^k.$$

9

Hence by choosing $\mathbf{v} = \phi^{k+1}$, (4.2) becomes

$$\frac{1}{\Delta t}\left(\phi^{k+1} - \phi^k, \phi^{k+1}\right) + \|\phi^{k+1}\|_A^2 + \left(B\phi^k, \phi^{k+1}\right)$$
$$= -\frac{1}{\Delta t}\left(\boldsymbol{\eta}^{k+1} - \boldsymbol{\eta}^k, \phi^{k+1}\right) - \left(\mathbf{r}^{k+1}, \phi^{k+1}\right) - \left(A\boldsymbol{\eta}^{k+1}, \phi^{k+1}\right)$$
$$- \left(B\boldsymbol{\eta}^k, \phi^{k+1}\right) - \left(B(\mathbf{u}(t^{k+1}) - \mathbf{u}(t^k)), \phi^{k+1}\right).$$

The first term on the LHS is bounded below as in the proof of Lemma 3.1. Add $\alpha\|\phi^{k+1}\|^2$ to both sides, and apply $\|\phi^{k+1}\|_A^2 + \alpha\|\phi^{k+1}\|^2 = \|\phi^{k+1}\|_{A+\alpha I}^2$. This results in a new bound

$$\frac{1}{2\Delta t}\left(\|\phi^{k+1}\|^2 - \|\phi^k\|^2\right) + \|\phi^{k+1}\|_{A+\alpha I}^2 + \left(B\phi^k, \phi^{k+1}\right)$$
$$\leq -\frac{1}{\Delta t}\left(\boldsymbol{\eta}^{k+1} - \boldsymbol{\eta}^k, \phi^{k+1}\right) - \left(\mathbf{r}^{k+1}, \phi^{k+1}\right) - \left(A\boldsymbol{\eta}^{k+1}, \phi^{k+1}\right) \tag{4.3}$$
$$- \left(B\boldsymbol{\eta}^k, \phi^{k+1}\right) - \left(B(\mathbf{u}(t^{k+1}) - \mathbf{u}(t^k)), \phi^{k+1}\right) + \alpha\|\phi^{k+1}\|^2.$$

The error terms involving the operator B must be absorbed into the $A + \alpha I$ norms. First split $\|\phi^{k+1}\|_{A+\alpha I}^2 = \frac{1}{2}\|\phi^{k+1}\|_{A+\alpha I}^2 + \frac{1}{2}\left(\|\phi^{k+1}\|_{A+\alpha I}^2 - \|\phi^k\|_{A+\alpha I}^2\right) + \frac{1}{2}\|\phi^k\|_{A+\alpha I}^2$. Then bound below $\left(B\phi^k, \phi^{k+1}\right) \geq -\frac{1}{2}\left(B\phi^{k+1}, \phi^{k+1}\right) - \frac{1}{2}\left(B\phi^k, \phi^k\right)$, so from (4.3) after multiplying through by 2 comes the bound

$$\frac{1}{\Delta t}\left(\|\phi^{k+1}\|^2 - \|\phi^k\|^2\right) + \|\phi^{k+1}\|_{A+\alpha I-B}^2 + \|\phi^k\|_{A+\alpha I-B}^2$$
$$+ \left(\|\phi^{k+1}\|_{A+\alpha I}^2 - \|\phi^k\|_{A+\alpha I}^2\right) \leq -\frac{2}{\Delta t}\left(\boldsymbol{\eta}^{k+1} - \boldsymbol{\eta}^k, \phi^{k+1}\right) \tag{4.4}$$
$$- 2\left(\mathbf{r}^{k+1}, \phi^{k+1}\right) - 2\left(A\boldsymbol{\eta}^{k+1}, \phi^{k+1}\right) - 2\left(B\boldsymbol{\eta}^k, \phi^{k+1}\right)$$
$$- 2\left(B(\mathbf{u}(t^{k+1}) - \mathbf{u}(t^k)), \phi^{k+1}\right) + 2\alpha\|\phi^{k+1}\|^2.$$

The right hand side of (4.4) must be bounded in a suitable way. The first two terms require only Hölder's and Young's inequalities to bound as

$$-\frac{2}{\Delta t}\left(\boldsymbol{\eta}^{k+1} - \boldsymbol{\eta}^k, \phi^{k+1}\right) - 2\left(\mathbf{r}^{k+1}, \phi^{k+1}\right) \leq \left\|\frac{\boldsymbol{\eta}^{k+1} - \boldsymbol{\eta}^k}{\Delta t}\right\|^2 + \|\mathbf{r}^{k+1}\|^2 + 2\|\phi^{k+1}\|^2. \tag{4.5}$$

The remaining three terms in (4.4) require special treatment. Using (2.1), apply Hölder's inequality to derive the first of the necessary bounds.

$$-2\left(A\boldsymbol{\eta}^{k+1}, \phi^{k+1}\right) = -2\sum_{i=1,2}\left\{\nu_i \int_{\Omega_i} \nabla\boldsymbol{\eta}_i^{k+1} \cdot \nabla\phi_{h,i}^{k+1}\, dx\right\}$$
$$\leq \sum_{i=1,2} \nu_i \left\{\int_{\Omega_i} |\nabla\boldsymbol{\eta}_i^{k+1}|^2\, dx\right\}^{1/2} \left\{\int_{\Omega_i} |\nabla\phi_{h,i}^{k+1}|^2\, dx\right\}^{1/2}$$
$$\leq C(\nu_1, \nu_2)\|\boldsymbol{\eta}^{k+1}\|_X\|\phi^{k+1}\|_X.$$

Applying Lemma 2.2, note that $\|\phi^{k+1}\|_X \leq C\|\phi^{k+1}\|_{A+\alpha I-B}$. Then use Young's inequality to get the bound

$$-2\left(A\boldsymbol{\eta}^{k+1}, \phi^{k+1}\right) \leq C\|\boldsymbol{\eta}^{k+1}\|_X\|\phi^{k+1}\|_{A+\alpha I-B}$$
$$\leq C\|\boldsymbol{\eta}^{k+1}\|_X^2 + \frac{1}{12}\|\phi^{k+1}\|_{A+\alpha I-B}^2. \tag{4.6}$$

10

The two remaining terms in (4.4) requiring bounds are treated in the same way. In general, for $\boldsymbol{\phi} = (\phi_1, \phi_2) \in X$ and $\boldsymbol{\psi} = (\psi_1, \psi_2) \in X_h$, bound the term $-2\left(B\boldsymbol{\phi}, \boldsymbol{\psi}\right)$ as follows. Note that, by (2.2),

$$-2\left(B\boldsymbol{\phi}, \boldsymbol{\psi}\right) = \kappa \int_I (\phi_1 - \phi_2)(\psi_1 - \psi_2)\, ds \leq \kappa \left\{ \int_I |\phi_1 - \phi_2|^2\, ds \right\}^{1/2} \left\{ \int_I |\psi_1 - \psi_2|^2\, ds \right\}^{1/2}.$$

From the proof of Lemma 2.2 it is clear these two last terms can be bounded above in the norm $\|\cdot\|_X$. Furthermore, Lemma 2.2 also implies

$$-2\left(B\boldsymbol{\phi}, \boldsymbol{\psi}\right) \leq C(\kappa, \Omega_1, \Omega_2)\, \|\boldsymbol{\phi}\|_X \|\boldsymbol{\psi}\|_X \leq C\, \|\boldsymbol{\phi}\|_X \|\boldsymbol{\psi}\|_{A+\alpha I - B}$$

$$\leq C\, \|\boldsymbol{\phi}\|_X^2 + \frac{1}{12}\|\boldsymbol{\psi}\|_{A+\alpha I - B}^2. \tag{4.7}$$

Hence by taking $\boldsymbol{\psi} = \boldsymbol{\phi}^{k+1}$ and either $\boldsymbol{\phi} = \mathbf{u}(t^{k+1}) - \mathbf{u}(t^k)$ or $\boldsymbol{\phi} = \boldsymbol{\eta}^k$ in (4.7) provides the needed bounds for (4.4). Combine results (4.5)–(4.7) to derive the new bound from (4.4) given by

$$\frac{1}{\Delta t}\left(\|\boldsymbol{\phi}^{k+1}\|^2 - \|\boldsymbol{\phi}^k\|^2 \right) + \|\boldsymbol{\phi}^{k+1}\|_{A+\alpha I - B}^2 + \|\boldsymbol{\phi}^k\|_{A+\alpha I - B}^2$$

$$+ \left(\|\boldsymbol{\phi}^{k+1}\|_{A+\alpha I}^2 - \|\boldsymbol{\phi}^k\|_{A+\alpha I}^2 \right) \leq \left\| \frac{\boldsymbol{\eta}^{k+1} - \boldsymbol{\eta}^k}{\Delta t} \right\|^2 + \|\mathbf{r}^{k+1}\|^2 \tag{4.8}$$

$$+ 2(1+\alpha)\|\boldsymbol{\phi}^{k+1}\|^2 + C\, \|\boldsymbol{\eta}^{k+1}\|_X^2 + C\, \|\mathbf{u}(t^{k+1}) - \mathbf{u}(t^k)\|_X^2$$

$$+ C\, \|\boldsymbol{\eta}^k\|_X^2 + \frac{3}{12}\|\boldsymbol{\phi}^{k+1}\|_{A+\alpha I - B}^2.$$

Now the last term on the RHS of (4.8) is subsumed. After multiplying through by Δt and summing over $k = 0, 1, 2, \cdots, n$ it follows

$$\|\boldsymbol{\phi}_h^{n+1}\|^2 + \Delta t\|\boldsymbol{\phi}_h^{n+1}\|_{A+\alpha I}^2 + \frac{3\Delta t}{4}\sum_{k=0}^{n}\|\boldsymbol{\phi}^{k+1}\|_{A+\alpha I - B}^2 + \Delta t \sum_{k=0}^{n}\|\boldsymbol{\phi}^k\|_{A+\alpha I - B}^2$$

$$\leq \|\boldsymbol{\phi}_h^0\|^2 + \Delta t\|\boldsymbol{\phi}_h^0\|_{A+\alpha I}^2 + \Delta t \sum_{k=0}^{n} \left\{ \left\| \frac{\boldsymbol{\eta}^{k+1} - \boldsymbol{\eta}^k}{\Delta t} \right\|^2 + \|\mathbf{r}^{k+1}\|^2 \right\} \tag{4.9}$$

$$+ 2(1+\alpha)\,\Delta t \sum_{k=0}^{n}\|\boldsymbol{\phi}^{k+1}\|^2 + C\,\Delta t \sum_{k=0}^{n} \left\{ \|\boldsymbol{\eta}^{k+1}\|_X^2 + \|\mathbf{u}(t^{k+1}) - \mathbf{u}(t^k)\|_X^2 + \|\boldsymbol{\eta}^k\|_X^2 \right\}.$$

The discrete Gronwall lemma may be applied to (4.9). Then combining repeated terms in the sums, a simplified bound follows:

$$\|\boldsymbol{\phi}_h^{n+1}\|^2 + \Delta t\|\boldsymbol{\phi}_h^{n+1}\|_{A+\alpha I}^2 + \frac{3\Delta t}{4}\sum_{k=0}^{n+1}\|\boldsymbol{\phi}^k\|_{A+\alpha I - B}^2$$

$$\leq e^{C_2(\alpha)T}\Bigg\{ \|\boldsymbol{\phi}_h^0\|^2 + \Delta t\|\boldsymbol{\phi}_h^0\|_{A+\alpha I}^2 + C\,\Delta t \sum_{k=0}^{n+1}\|\boldsymbol{\eta}^k\|_X^2 \tag{4.10}$$

$$+ \Delta t \sum_{k=0}^{n} \left\{ \left\| \frac{\boldsymbol{\eta}^{k+1} - \boldsymbol{\eta}^k}{\Delta t} \right\|^2 + \|\mathbf{r}^{k+1}\|^2 + C\, \|\mathbf{u}(t^{k+1}) - \mathbf{u}(t^k)\|_X^2 \right\} \Bigg\},$$

with $C_2(\alpha) = 2(1+\alpha)(1 - 2\Delta t(1+\alpha))^{-1}$. Bounds for the last three terms in (4.10) can be

11

derived using well known arguments [18, 19]. Indeed, the following inequalities hold:

$$\Delta t \sum_{k=0}^{n} \left\| \frac{\boldsymbol{\eta}^{k+1} - \boldsymbol{\eta}^k}{\Delta t} \right\|^2 \leq \int_0^{t^{n+1}} \|\boldsymbol{\eta}_t\|^2 \, dt \leq \|\boldsymbol{\eta}_t\|^2_{L^2(0,T;L^2(\Omega))}$$

$$\Delta t \sum_{k=0}^{n} \|\mathbf{u}(t^{k+1}) - \mathbf{u}(t^k)\|^2_X \leq \Delta t^2 \int_0^{t^{n+1}} \|\mathbf{u}_t\|^2_X \, dt \leq \Delta t^2 \|\mathbf{u}_t\|^2_{L^2(0,T;X)} \qquad (4.11)$$

$$\Delta t \sum_{k=0}^{n} \|\mathbf{r}^{k+1}\|^2 \leq \frac{\Delta t^2}{3} \int_0^{t^{n+1}} \|\mathbf{u}_{tt}\|^2 \, dt \leq \frac{\Delta t^2}{3} \|\mathbf{u}_{tt}\|^2_{L^2(0,T;L^2(\Omega))} \, .$$

Apply the triangle inequality to $\|\boldsymbol{\phi}_h^0\|^2 + \Delta t \|\boldsymbol{\phi}_h^0\|^2_{A+\alpha I}$. Recall $\boldsymbol{\eta}^k = \mathbf{u}(t^k) - \mathbf{v}^k$ with $\mathbf{v}^k \in X_h$ arbitrarily chosen, so take the infimum over $\mathbf{v}^k \in X_h$ on the RHS. Combined with the inequalities in (4.11) it follows

$$\|\boldsymbol{\phi}_h^{n+1}\|^2 + \Delta t \|\boldsymbol{\phi}_h^{n+1}\|^2_{A+\alpha I} + \frac{3\Delta t}{4} \sum_{k=0}^{n+1} \|\boldsymbol{\phi}^k\|^2_{A+\alpha I - B}$$

$$\leq C_1^* e^{C_2(\alpha)T} \bigg\{ \|\mathbf{u}(0) - \mathbf{u}^0\|^2 + \Delta t \|\mathbf{u}(0) - \mathbf{u}^0\|^2_{A+\alpha I}$$

$$+ \inf_{v_h^0 \in X_h} \left\{ \|\boldsymbol{\eta}^0\|^2 + \Delta t \|\boldsymbol{\eta}^0\|^2_{A+\alpha I} \right\} \qquad (4.12)$$

$$+ \inf_{\mathbf{v}^k \in X_h} \|\boldsymbol{\eta}^k\|^2_X + \inf_{\mathbf{v} \in X_h} \|\boldsymbol{\eta}_t\|^2_{L^2(0,T;L^2(\Omega))}$$

$$+ \Delta t^2 \left(\|\mathbf{u}_t\|^2_{L^2(0,T;X)} + \|\mathbf{u}_{tt}\|^2_{L^2(0,T;L^2(\Omega))} \right) \bigg\} .$$

Lemma 2.2 can now be applied to replace all norms of type $\|\cdot\|_{A+\alpha I - B}$ and $\|\cdot\|_{A+\alpha I}$ with the norm $\|\cdot\|_X$. Bound above $\Delta t \inf_{\mathbf{v}^k \in X_h} \sum_{k=0}^{n+1} \|\eta^k\|^2_X \leq T \max_{k=0,2,\cdots,n+1} \inf_{\mathbf{v}^k \in X_h} \|\eta^k\|^2_X$. One more application of the triangle inequality and rearranging constants yields the final result.
□

In Algorithm 2.2 no time-step restriction is needed if $\kappa \leq \gamma \min\{\nu_1, \nu_2\}$, for some positive constant $\gamma = \gamma(\Omega_1, \Omega_2)$. The case of larger κ is less clear. For large κ the analysis indicates that convergence will require $\Delta t \leq O(\frac{\min\{\nu_1,\nu_2\}}{\kappa^2})$ and the error might grow as fast as e^{κ^2}, so that computations for $\kappa >> 1$ may require very small meshes and large numbers of time steps unless $\min\{\nu_1, \nu_2\} >> \kappa$.

The proof of convergence for Algorithm 2.3 is technically simpler, and shows optimal convergence in $L^2(0,T; H^1)$ with no time step restriction. κ should have only a small effect on error for the implicit method, while error of the partitioned method may increase proportional to κ, Theorem 4.2 next.

THEOREM 4.2. *(Convergence of the data-passing partitioned scheme)*

Let $\mathbf{u}(t; x) \in X$ *for all* $t \in (0, T)$ *solve (1.1)–(1.4), such that* $\mathbf{u}_t \in L^2(0,T; X)$ *and* $\mathbf{u}_{tt} \in L^2(0,T; L^2(\Omega))$. *Then* $\exists C > 0$ *independent of* h, Δt *such that for any* $n \in \{0, 1, 2, \cdots, M - 1 = \frac{T}{\Delta t} - 1\}$, *the solution* $\mathbf{u}^{n+1} \in X_h$ *of (2.11) satisfies:*

$$\|\mathbf{u}(t^{n+1}) - \mathbf{u}^{n+1}\|^2 + \kappa \Delta t \|\mathbf{u}(t^{n+1}) - \mathbf{u}^{n+1}\|^2_I + \sum_{k=0}^{n} \|\mathbf{u}(t^{k+1}) - \mathbf{u}^{k+1}\|^2_X$$

$$\leq C \bigg\{ \|\mathbf{u}(0) - \mathbf{u}^0\|^2 + \kappa \Delta t \|\mathbf{u}(0) - \mathbf{u}^0\|^2_I + \Delta t^2 \|\mathbf{u}_t\|^2_{L^2(0,T;X)} + \Delta t^2 \|\mathbf{u}_{tt}\|^2_{L^2(0,T;L^2(\Omega))}$$

$$+ \inf_{\mathbf{v}^0 \in X_h} \left\{ \|\mathbf{u}(0) - \mathbf{v}^0\|^2 + \Delta t \|\mathbf{u}(0) - \mathbf{v}^0\|^2_X \right\} + \inf_{\mathbf{v} \in X_h} \|(\mathbf{u}(0) - \mathbf{v})_t\|^2$$

$$+ T \max_{k=1,2,\cdots,n+1} \inf_{\mathbf{v}^k \in X_h} \|\mathbf{u}(t^k) - \mathbf{v}^k\|^2_X \bigg\} .$$

12

Proof. Restricting test functions to X_h, subtract (2.11) from (1.6), to get the error equation:

$$\left(\mathbf{u}_t(t^{k+1}) - \frac{\mathbf{u}^{k+1} - \mathbf{u}^k}{\Delta t}, \mathbf{v}\right) + \left(A(\mathbf{u}(t^{k+1}) - \mathbf{u}^{k+1}), \mathbf{v}\right) + \kappa \int_I [\mathbf{u}(t^{k+1})][\mathbf{v}]\, ds$$
$$- \kappa \int_I (u_1^{k+1} - u_2^k) v_1\, ds - \kappa \int_I (u_2^{k+1} - u_1^k) v_2\, ds = 0.$$

Define $\mathbf{r}^{k+1} = \mathbf{u}_t(t^{k+1}) - \frac{\mathbf{u}(t^{k+1}) - \mathbf{u}(t^k)}{\Delta t}$ and rearrange terms.

$$\left(\mathbf{r}^{k+1}, \mathbf{v}\right) + \left(\frac{\mathbf{u}(t^{k+1}) - \mathbf{u}^{k+1}}{\Delta t} - \frac{\mathbf{u}(t^k) - \mathbf{u}^k}{\Delta t}, \mathbf{v}\right) + \left(A(\mathbf{u}(t^{k+1}) - \mathbf{u}^{k+1}), \mathbf{v}\right) + \kappa \int_I [\mathbf{u}(t^{k+1})][\mathbf{v}]\, ds$$
$$- \kappa \int_I (u_1^{k+1} - u_2^k) v_1\, ds - \kappa \int_I (u_2^{k+1} - u_1^k) v_2\, ds = 0, \ \forall \mathbf{v} \in X_h.$$

Define for each $k = 0, 1, 2, \cdots$ the functions $(\mathbf{u}(t^k) - \mathbf{v}^k) + (\mathbf{v}^k - \mathbf{u}^k) = \boldsymbol{\eta}^k + \boldsymbol{\phi}^k$, where $\mathbf{v}^k \in X_h$ is arbitrary. Then by adding and subtracting $\mathbf{v}^k$ where appropriate,

$$\frac{1}{\Delta t}\left(\boldsymbol{\phi}^{k+1} - \boldsymbol{\phi}^k, \mathbf{v}\right) + \left(A\boldsymbol{\phi}^{k+1}, \mathbf{v}\right) + \kappa \int_I [\mathbf{u}(t^{k+1})][\mathbf{v}]\, ds$$
$$- \kappa \int_I (u_1^{k+1} - u_2^k) v_1\, ds - \kappa \int_I (u_2^{k+1} - u_1^k) v_2\, ds \tag{4.13}$$
$$= -\frac{1}{\Delta t}\left(\boldsymbol{\eta}^{k+1} - \boldsymbol{\eta}^k, \mathbf{v}\right) - \left(\mathbf{r}^{k+1}, \mathbf{v}\right) - \left(A\boldsymbol{\eta}^{k+1}, \mathbf{v}\right), \ \forall \mathbf{v} \in X_h.$$

Choosing $\mathbf{v} = \boldsymbol{\phi}^{k+1}$, (4.13) becomes

$$\frac{1}{\Delta t}\left(\boldsymbol{\phi}^{k+1} - \boldsymbol{\phi}^k, \boldsymbol{\phi}^{k+1}\right) + \|\boldsymbol{\phi}^{k+1}\|_A^2 + \kappa \int_I [\mathbf{u}(t^{k+1})][\boldsymbol{\phi}^{k+1}]\, ds$$
$$- \kappa \int_I (u_1^{k+1} - u_2^k)\phi_1^{k+1}\, ds - \kappa \int_I (u_2^{k+1} - u_1^k)\phi_2^{k+1}\, ds$$
$$= -\frac{1}{\Delta t}\left(\boldsymbol{\eta}^{k+1} - \boldsymbol{\eta}^k, \boldsymbol{\phi}^{k+1}\right) - \left(\mathbf{r}^{k+1}, \boldsymbol{\phi}^{k+1}\right) - \left(A\boldsymbol{\eta}^{k+1}, \boldsymbol{\phi}^{k+1}\right).$$

The first term on the LHS is bounded below as in the proof of Lemma 3.1, yielding the new bound

$$\frac{1}{2\Delta t}\left(\|\boldsymbol{\phi}^{k+1}\|^2 - \|\boldsymbol{\phi}^k\|^2\right) + \|\boldsymbol{\phi}^{k+1}\|_A^2 + \kappa \int_I [\mathbf{u}(t^{k+1})][\boldsymbol{\phi}^{k+1}]\, ds$$
$$- \kappa \int_I (u_1^{k+1} - u_2^k)\phi_1^{k+1}\, ds - \kappa \int_I (u_2^{k+1} - u_1^k)\phi_2^{k+1}\, ds \tag{4.14}$$
$$\leq -\frac{1}{\Delta t}\left(\boldsymbol{\eta}^{k+1} - \boldsymbol{\eta}^k, \boldsymbol{\phi}^{k+1}\right) - \left(\mathbf{r}^{k+1}, \boldsymbol{\phi}^{k+1}\right) - \left(A\boldsymbol{\eta}^{k+1}, \boldsymbol{\phi}^{k+1}\right).$$

The interface terms must be handled in a useful way. Algebraically rearranging terms, adding and subtracting $u_1(t^k), u_2(t^k)$ to retain first order accuracy in time it follows

$$\kappa \int_I [\mathbf{u}(t^{k+1})][\boldsymbol{\phi}^{k+1}]\, ds - \kappa \int_I (u_1^{k+1} - u_2^k)\phi_1^{k+1}\, ds - \kappa \int_I (u_2^{k+1} - u_1^k)\phi_2^{k+1}\, ds$$
$$= \kappa \int_I (\mathbf{u}(t^{k+1}) - \mathbf{u}^{k+1}) \cdot \boldsymbol{\phi}^{k+1}\, ds - \kappa \int_I (u_2(t^{k+1}) - u_2(t^k))\phi_1^{k+1}\, ds \tag{4.15}$$
$$- \kappa \int_I (u_1(t^{k+1}) - u_1(t^k))\phi_2^{k+1}\, ds - \kappa \int_I (u_2(t^k) - u_2^k)\phi_1^{k+1}\, ds - \kappa \int_I (u_1(t^k) - u_1^k)\phi_2^{k+1}\, ds.$$

13

Now expand (4.15) by substituting $\mathbf{u}(t^j) - \mathbf{u}^j = \boldsymbol{\eta}^j + \boldsymbol{\phi}^j$ where $j = k, k+1$,

$$\kappa \int_I [\mathbf{u}(t^{k+1})][\boldsymbol{\phi}^{k+1}] \, ds - \kappa \int_I (u_1^{k+1} - u_2^k)\phi_1^{k+1} \, ds - \kappa \int_I (u_2^{k+1} - u_1^k)\phi_2^{k+1} \, ds$$

$$= \kappa \|\boldsymbol{\phi}^{k+1}\|_I^2 + \kappa \int_I \boldsymbol{\eta}^{k+1} \cdot \boldsymbol{\phi}^{k+1} \, ds - \kappa \int_I (u_2(t^{k+1}) - u_2(t^k))\phi_1^{k+1} \, ds$$

$$- \kappa \int_I (u_1(t^{k+1}) - u_1(t^k))\phi_2^{k+1} \, ds - \kappa \int_I \eta_2^k \phi_1^{k+1} \, ds - \kappa \int_I \phi_2^k \phi_1^{k+1} \, ds \qquad (4.16)$$

$$- \kappa \int_I \eta_1^k \phi_2^{k+1} \, ds - \kappa \int_I \phi_1^k \phi_2^{k+1} \, ds \,.$$

Substitution of (4.16) into (4.14) provides a more useful expression to bound $\boldsymbol{\phi}^{k+1}$. After rearranging terms,

$$\frac{1}{2\Delta t}\left(\|\boldsymbol{\phi}^{k+1}\|^2 - \|\boldsymbol{\phi}^k\|^2\right) + \|\boldsymbol{\phi}^{k+1}\|_A^2 + \kappa \|\boldsymbol{\phi}^{k+1}\|_I^2 \leq -\frac{1}{\Delta t}\left(\boldsymbol{\eta}^{k+1} - \boldsymbol{\eta}^k, \boldsymbol{\phi}^{k+1}\right)$$

$$- \left(\mathbf{r}^{k+1}, \boldsymbol{\phi}^{k+1}\right) - \left(A\boldsymbol{\eta}^{k+1}, \boldsymbol{\phi}^{k+1}\right) - \kappa \int_I \boldsymbol{\eta}^{k+1} \cdot \boldsymbol{\phi}^{k+1} \, ds$$

$$+ \kappa \int_I (u_1(t^{k+1}) - u_1(t^k))\phi_2^{k+1} \, ds + \kappa \int_I (u_2(t^{k+1}) - u_2(t^k))\phi_1^{k+1} \, ds \qquad (4.17)$$

$$+ \kappa \int_I \eta_2^k \phi_1^{k+1} \, ds + \kappa \int_I \phi_2^k \phi_1^{k+1} \, ds + \kappa \int_I \eta_1^k \phi_2^{k+1} \, ds + \kappa \int_I \phi_1^k \phi_2^{k+1} \, ds.$$

The right hand side of (4.17) must be bounded in a suitable way. The first three terms are the same as in (4.5) and are treated the same way. In fact most of the remaining proof is similar to that of Theorem 4.1, apart from properly bounding the interface terms. All but two of these terms contain some factor known to be $O(h)$ or $O(\Delta t)$, so Young's inequality is applied:

$$\kappa \int_I (u_i(t^{k+1}) - u_i(t^k))\phi_j^{k+1} \, ds \leq \kappa \|u_i(t^{k+1}) - u_i(t^k)\|_I \|\phi_j^{k+1}\|_I$$

$$\leq C(\Omega_j, \nu_j, \kappa)\|u_i(t^{k+1}) - u_i(t^k)\|_I \left(\nu_j^{1/2}\|\nabla \phi_j^{k+1}\|_{\Omega_j}\right)$$

$$\leq C(\Omega_j, \nu_j, \kappa^2, \epsilon)\|u_i(t^{k+1}) - u_i(t^k)\|_I^2 + \frac{\epsilon}{2}\nu_j\|\nabla \phi_j^{k+1}\|_{\Omega_j}^2$$

$$\kappa \int_I \eta_i^{k+1} \phi_j^{k+1} \, ds \leq \kappa \|\eta_i^{k+1}\|_I \|\phi_j^{k+1}\|_I \leq C(\Omega_j, \nu_j, \kappa)\|\eta_i^{k+1}\|_I \left(\nu_j^{1/2}\|\nabla \phi_j^{k+1}\|_{\Omega_j}\right)$$

$$\leq C(\Omega_j, \nu_j, \kappa^2, \epsilon)\|\eta_i^{k+1}\|_I^2 + \frac{\epsilon}{2}\nu_j\|\nabla \phi_j^{k+1}\|_{\Omega_j}^2 \,,$$

where ϵ is chosen small enough so that all terms occurring on the RHS of (4.17) of the form $\frac{\epsilon}{2}\nu_j\|\nabla \phi_j^{k+1}\|_{\Omega_j}^2$ may be added so as not to exceed $\frac{1}{2}\|\boldsymbol{\phi}^{k+1}\|_A^2$. This leaves only two interface terms to bound. Applying Hölder's and Young's inequalities to these, the bounds

$$\kappa \int_I \phi_1^k \phi_2^{k+1} \, ds + \kappa \int_I \phi_2^k \phi_1^{k+1} \, ds \leq \frac{1}{2}\|\boldsymbol{\phi}^{k+1}\|_I^2 + \frac{1}{2}\|\boldsymbol{\phi}^k\|_I^2 \,,$$

are applied and subtract both of these terms to the LHS of (4.17) to get the new expression

$$\frac{1}{2\Delta t}\left(\|\boldsymbol{\phi}^{k+1}\|^2 - \|\boldsymbol{\phi}^k\|^2\right) + \frac{1}{2}\|\boldsymbol{\phi}^{k+1}\|_A^2 + \frac{\kappa}{2}\left(\|\boldsymbol{\phi}^{k+1}\|_I^2 - \|\boldsymbol{\phi}^k\|_I^2\right)$$

$$\leq C\Big\{\|\frac{\boldsymbol{\eta}^{k+1} - \boldsymbol{\eta}^k}{\Delta t}\|^2 + \|\mathbf{r}^{k+1}\|^2 + \|\nabla \boldsymbol{\eta}^{k+1}\|^2 + \|\boldsymbol{\eta}^{k+1}\|_I^2 + \|\boldsymbol{\eta}^k\|_I^2 \qquad (4.18)$$

$$+ \|\mathbf{u}(t^{k+1}) - \mathbf{u}(t^k)\|_I^2\Big\} \,.$$

Multiply through (4.18) by $2\Delta t$ and sum over $k = 0, 1, \cdots, n$ to derive a bound of the form

$$
\begin{aligned}
\|\phi^{n+1}\|^2 &+ \kappa\Delta t\|\phi^{n+1}\|_I^2 + \Delta t \sum_{k=0}^{n}\|\phi^{k+1}\|_A^2 \\
&\leq \|\phi^0\|^2 + \kappa\Delta t\|\phi^0\|_I^2 + C\Delta t \sum_{k=0}^{n}\left\{\|\frac{\boldsymbol{\eta}^{k+1} - \boldsymbol{\eta}^k}{\Delta t}\|^2 + \|\mathbf{r}^{k+1}\|^2 \right. \\
&\left. + \|\nabla\boldsymbol{\eta}^{k+1}\|^2 + \|\boldsymbol{\eta}^{k+1}\|_I^2 + \|\boldsymbol{\eta}^k\|_I^2 + \|\mathbf{u}(t^{k+1}) - \mathbf{u}(t^k)\|_I^2 \right\}.
\end{aligned}
\tag{4.19}
$$

As an application of the Trace Theorem, note that

$$
\|\mathbf{u}(t^{k+1}) - \mathbf{u}(t^k)\|_I^2 \leq C \|\mathbf{u}(t^{k+1}) - \mathbf{u}(t^k)\|_X^2
$$
$$
\|\boldsymbol{\eta}^k\|_I^2 \leq C \|\boldsymbol{\eta}^k\|_X^2 .
$$

The rest of the proof follows as for Theorem 4.1. The norm $\|\cdot\|_A$ is replaced with $\|\cdot\|_X$ after applying Lemma 2.2 with $\alpha = 0$. Application of the bounds (4.11) and the triangle inequality finishes the proof. □

COROLLARY 4.3. *Let $X_h \subset X$ be a finite element space corresponding to continuous piece-wise polynomials of degree k. If $\mathbf{u}(\cdot, t)$ is a solution of (1.1)–(1.4) satisfying the assumptions of Theorem 4.1, (respectively Theorem 4.2) and $\mathbf{u}^0$ approximates $\mathbf{u}(\cdot, 0)$ such that*

$$
\|\mathbf{u}(\cdot, 0) - \mathbf{u}^0\| = O(h^q),
$$

then the corresponding approximations (2.9) and (2.11) converge at the rate $O(\Delta t + h^q)$ in the norm

$$
\left\{\Delta t \sum_{k=0}^{M}\|\mathbf{u}(t^k) - \mathbf{u}^k\|_X^2\right\}^{1/2} .
$$

Proof. Applying the results of the respective theorems this follows from finite element analysis, (e.g. [18, 19]). Indeed, the result follows from applying the following interpolation error estimates for $\phi \in X$.

$$
\inf_{\mathbf{v} \in X_h} \|\phi - \mathbf{v}\| \leq C\,h^{k+1}\|\phi\|_{W^{k+1}(\Omega)}
$$
$$
\inf_{\mathbf{v} \in X_h} \|\phi - \mathbf{v}\|_X \leq C\,h^k\|\phi\|_{W^{k+1}(\Omega)}
$$
$$
\inf_{\mathbf{v} \in X_h} \|(\phi - \mathbf{v})_t\| \leq C\,h^{k+1}\|\phi_t\|_{W^{k+1}(\Omega)} .
$$

□

5. Computational Testing. This section investigates the two methods of uncoupling the subdomain problems given in Algorithms 2.2 and 2.3, the IMEX approach (2.9) and the data passing partitioned approach (2.11). We also solve the fully coupled, monolithic problem (2.5) and use its solution as a baseline for comparison. In Section 5.1, the predicted rates of convergence are verified for the two (plus fully implicit) methods on two problems. In Section 5.2, computational issues related to dependence of the methods stability and accuracy on the paramters κ, ν_1, and ν_2 are studied. In Section 5.3, a brief discussion and a numerical example of a second-order IMEX scheme is presented.

5.1. Convergence Rate Verification. Assume $\Omega_1 = [0, 1] \times [0, 1]$ and $\Omega_2 = [0, 1] \times [-1, 0]$, so I is the portion of the x-axis from 0 to 1. Then $\mathbf{n}_1 = [0, -1]^T$ and $\mathbf{n}_2 = [0, 1]^T$. For a, ν_1, ν_2, and κ all arbitrary positive constants, the right hand side function $\mathbf{f}$ is chosen to ensure that

$$
u_1(t, x, y) = ax(1 - x)(1 - y)e^{-t}
$$
$$
u_2(t, x, y) = ax(1 - x)(c_1 + c_2 y + c_3 y^2)e^{-t} .
$$

15

The constants c_1, c_2, c_3 are determined from the interface conditions (1.2) and the boundary conditions for u_2. One may verify that with the following choices for c_1, c_2, c_3, u_1 and u_2 will satisfy (1.1)–(1.4) with $g_1 = g_2 = 0$, i. e. when $x \in \{0, 1\}$ or $y \in \{-1, 1\}$:

$$c_1 = 1 + \frac{\nu_1}{\kappa} \, , \ c_2 = \frac{-\nu_1}{\nu_2} \, , \ c_3 = c_2 - c_1.$$

The numerical analysis performed in Section 4 indicates that by choosing κ to be no larger than ν_1, ν_2 the IMEX scheme should perform as well as the implicit scheme. Computational results comparing the performance of the two methods are listed for two test problems:
- Test Problem 1: $a = \nu_1 = \nu_2 = \kappa = 1$.
- Test Problem 2: $a = 4, \nu_1 = 5, \nu_2 = 10, \kappa = 1/4$.

A plot of the approximation computed by the implicit method at $T = 1$ for test problem 1 is given in Figure 5.1.
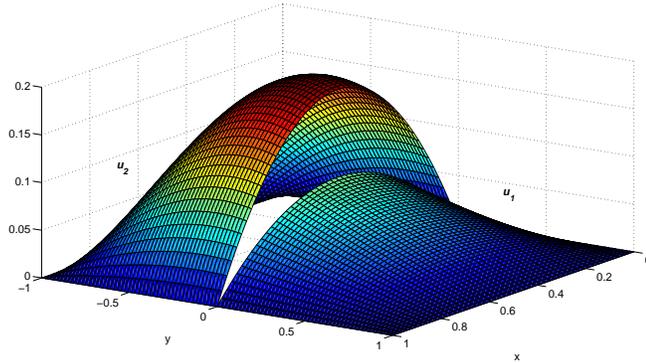

FIG. 5.1. *Implicit approximation at $T = 1$, Test Problem 1.*

For both problems, computations were performed using the implicit, partition, and IMEX schemes with finite element spaces consisting of continuous piece-wise polynomials of degree 1. The code was implemented using the software package `FreeFEM++` [12]. By choosing $\Delta t = h$ the expected convergence rate of $O(\Delta t)$ was achieved by all algorithms for these two test problems. In the following tables, the norm $\|\mathbf{u}\|$ is the discrete $L^2(0, T; H^1(\Omega))$ norm, given by

$$\|\mathbf{u}\| = \left(\sum_{n=1}^{N} \Delta t |\mathbf{u}(t_n)|_{H^1(\Omega)} \right)^{1/2} \, ,$$

where $N = T/\Delta t$ and $| \cdot |_{H^1(\Omega)}$ is the $H^1(\Omega)$ spatial seminorm. Tables 5.1 and 5.2 give the errors produced by each of the methods, showing that for these choices of parameters, all three methods compute solutions to very similar levels of accuracy.

The IMEX scheme lags the interface term, and the theory indicates that numerical difficulties may occur if κ is too large, or if the jump $u_1 - u_2$ is large compared to the dissipation rates ν_1, ν_2. Computations for $\nu_1 = \nu_2 = 1$ were also performed while varying κ between 10^{-3} and 10^3, showing the implicit scheme converges optimally choosing $\Delta t = h$ in all cases. These calculations are omitted for brevity. The IMEX scheme fails to converge for $\kappa > 5$ when choosing $\Delta t = h$. For these parameter values the IMEX scheme is expected to require a condition on the time step as outlined in the proof of Theorem 4.1. This issue is further explored in Section 5.2.

In Figure 5.2, a plot of $\|\mathbf{u}\|$ computed by each of the solution methods for decreasing time step size is given. For these plots, $a = \nu_1 = \nu_2 = 1.0$ and $h = 1/64$. As the size of κ grows, is it observed that the stability of the IMEX method decreases.

16

h	Δt	$\|\mathbf{u}(t_n) - \mathbf{u}_{imp}^n\|$	rate	$\|u_1(t_n) - u_{1,imp}^n\|$	rate	$\|u_2(t_n) - u_{2,imp}^n\|$	rate
1/2	1/2	0.339237		0.0981878		0.324717	
1/4	1/4	0.189073	0.84	0.0629993	0.64	0.178269	0.87
1/8	1/8	0.10112	0.90	0.0345772	0.87	0.0950246	0.91
1/16	1/16	0.0522111	0.95	0.0179662	0.94	0.0490226	0.95
1/32	1/32	0.0265096	0.98	0.00913733	0.98	0.0248851	0.98
1/64	1/64	0.0133544	0.99	0.00460509	0.99	0.0125352	0.99

h	Δt	$\|\mathbf{u}(t_n) - \mathbf{u}_{part}^n\|$	rate	$\|u_1(t_n) - u_{1,part}^n\|$	rate	$\|u_2(t_n) - u_{2,part}^n\|$	rate
1/2	1/2	0.341323		0.103661		0.325201	
1/4	1/4	0.191544	0.83	0.0679054	0.61	0.179103	0.86
1/8	1/8	0.102654	0.90	0.0374796	0.86	0.0955673	0.91
1/16	1/16	0.0530381	0.95	0.0195048	0.94	0.0493214	0.95
1/32	1/32	0.0269361	0.98	0.00992551	0.97	0.0250407	0.98
1/64	1/64	0.0135707	0.99	0.00500371	0.99	0.0126145	0.99

h	Δt	$\|\mathbf{u}(t_n) - \mathbf{u}_{imex}^n\|$	rate	$\|u_1(t_n) - u_{1,imex}^n\|$	rate	$\|u_2(t_n) - u_{2,imex}^n\|$	rate
1/2	1/2	0.339893		0.0993662		0.325044	
1/4	1/4	0.189522	0.84	0.0639112	0.64	0.178421	0.87
1/8	1/8	0.101347	0.90	0.0350701	0.87	0.0950854	0.91
1/16	1/16	0.0523184	0.95	0.0182123	0.95	0.0490462	0.96
1/32	1/32	0.0265614	0.98	0.00926006	0.98	0.0248949	0.98
1/64	1/64	0.0133798	0.99	0.0046665	0.99	0.0125397	0.99

TABLE 5.1

Errors for computed approximations, test problem 1

h	Δt	$\|\mathbf{u}(t_n) - \mathbf{u}_{imp}^n\|$	rate	$\|u_1(t_n) - u_{1,imp}^n\|$	rate	$\|u_2(t_n) - u_{2,imp}^n\|$	rate
1/2	1/2	11.6344		0.393197		11.6277	
1/4	1/4	6.60502	0.82	0.252197	0.64	6.6002	0.82
1/8	1/8	3.53635	0.90	0.13829	0.87	3.53365	0.90
1/16	1/16	1.82584	0.95	0.071831	0.95	1.82443	0.95
1/32	1/32	0.926987	0.98	0.0365283	0.98	0.926267	0.98
1/64	1/64	0.466956	0.99	0.0184091	0.99	0.466593	0.99

h	Δt	$\|\mathbf{u}(t_n) - \mathbf{u}_{part}^n\|$	rate	$\|u_1(t_n) - u_{1,part}^n\|$	rate	$\|u_2(t_n) - u_{2,part}^n\|$	rate
1/2	1/2	11.6345		0.397053		11.6277	
1/4	1/4	6.6052	0.82	0.256811	0.63	6.60021	0.82
1/8	1/8	3.53648	0.90	0.14154	0.86	3.53365	0.90
1/16	1/16	1.82591	0.95	0.0736946	0.94	1.82443	0.95
1/32	1/32	0.927027	0.98	0.0375179	0.97	0.926267	0.98
1/64	1/64	0.466977	0.99	0.0189183	0.99	0.466593	0.99

h	Δt	$\|\mathbf{u}(t_n) - \mathbf{u}_{imex}^n\|$	rate	$\|u_1(t_n) - u_{1,imex}^n\|$	rate	$\|u_2(t_n) - u_{2,imex}^n\|$	rate
1/2	1/2	11.6345		0.39647		11.6277	
1/4	1/4	6.60517	0.82	0.256227	0.63	6.60019	0.82
1/8	1/8	3.53646	0.90	0.141173	0.86	3.53364	0.90
1/16	1/16	1.8259	0.95	0.0734932	0.94	1.82442	0.95
1/32	1/32	0.927021	0.98	0.037413	0.97	0.926266	0.98
1/64	1/64	0.466974	0.99	0.0188648	0.99	0.466593	0.99

TABLE 5.2

Errors for computed approximations, test problem 2

5.2. Relative Parameter Scaling. The computational results above imply the IMEX scheme will present an attractive alternative to the implicit scheme for problems where decoupling is necessary, so long as energy transfer across I is not too fast, i.e. except when $\kappa >> \min\{\nu_1, \nu_2\}$. To gain a more precise understanding of the time step requirements of the IMEX scheme, consider the case when κ is large compared to ν_2. This corresponds to a high flux of energy into Ω_2 with little diffusion, and thus lagging the interface term requires smaller time steps be taken to maintain stability and accuracy of the scheme. Referring to Theorem 4.1, note that choosing $\Delta t < (2 + 2\alpha)^{-1}$ should ensure optimal convergence. The size of α depends on the relative sizes of κ, ν_1, ν_2. From the proof of Lemma 2.2 if $\nu_1 = \nu_2 = 1$ it follows that $\alpha = C(\kappa^2)$, and thus the time step size for the IMEX scheme should scale like κ^{-2} for κ sufficiently large.

Using the test problem of Section 4.1 with $a = \nu_1 = \nu_2 = 1$ and $\kappa = 10$ and 100, calculations were performed with $\Delta t = h$, yielding no convergence, for mesh sizes as small as 1/32. For these mesh sizes, the value of Δt is not small enough compared to κ^{-2}. The computations were repeated for fixed $\Delta t = \frac{1}{2\kappa}$ and mesh sizes between 1/2 and 1/32, also yielding no convergence. However,
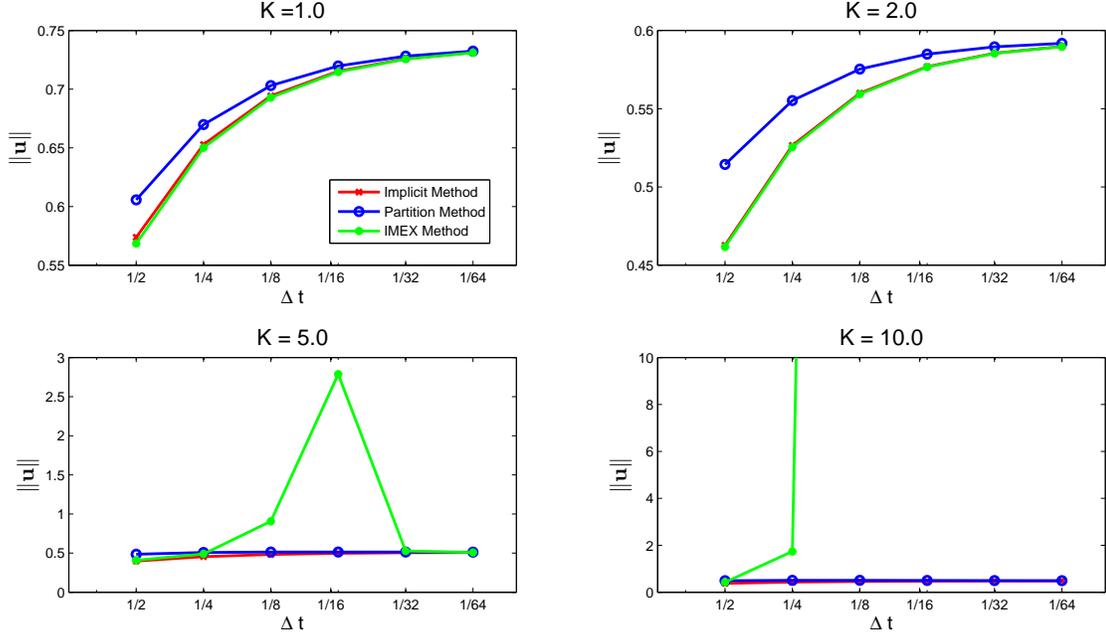
FIG. 5.2. *Stability of $\|\mathbf{u}\|$ as $\Delta t \to 0$, different values of κ.*

using the fixed time step size of $\Delta t = \frac{1}{2\kappa^2}$, optimal convergence was recovered as seen in Tables 5.3 and 5.4.

For the choice $\kappa = 10$, restricting $\Delta t < h^2$ is too restrictive, as seen by the error for the mesh size $h = 1/32$ in Table 5.3. For $\kappa = 100$, using the scaling $\Delta t < 0.5h^2$ is not restrictive enough, as shown in calculations omitted herein for brevity, on mesh sizes as small as $h = 1/32$. Computational evidence supports that for larger values of κ, the time step restriction scales like κ^{-2} and is not dependent on the mesh size.

h	Δt	$\|\mathbf{u}(t_n) - \mathbf{u}_{imex}^n\|$	rate	$\|u_1(t_n) - u_{1,imex}^n\|$	rate	$\|u_2(t_n) - u_{2,imex}^n\|$	rate
1/2	1/200	0.295741		0.129068		0.266090	
1/4	·	0.143322	1.045	0.071673	0.849	0.124113	1.100
1/8	·	0.071858	0.996	0.036765	0.963	0.061741	1.007
1/16	·	0.035947	0.999	0.018490	0.992	0.030827	1.002
1/32	·	0.017967	1.000	0.009255	0.998	0.015400	1.001

TABLE 5.3
IMEX convergence results for $\kappa = 10.0$, $\Delta t = (2\kappa^2)^{-1}$

h	Δt	$\|\mathbf{u}(t_n) - \mathbf{u}_{imex}^n\|$	rate	$\|u_1(t_n) - u_{1,imex}^n\|$	rate	$\|u_2(t_n) - u_{2,imex}^n\|$	rate
1/2	$\frac{1}{2 \cdot 10^4}$	0.283101		0.130035		0.251470	
1/4	·	0.137155	1.046	0.071969	0.853	0.116756	1.107
1/8	·	0.068752	0.996	0.036872	0.965	0.058029	1.009
1/16	·	0.034391	0.999	0.018537	0.992	0.028967	1.002
1/32	·	0.017189	1.001	0.009277	0.999	0.014471	1.001

TABLE 5.4
IMEX convergence results for $\kappa = 100.0$, $\Delta t = (2\kappa^2)^{-1}$

Theorem 4.2 predicts that no timestep restriction is required for convergence of the data passing partitioned time stepping method, but that error may increase proportional to κ. In Table 5.5 the computational results are listed for the partitioned method applied to the test problem with $a = \nu_1 = \nu_2 = 1$ and $\kappa = 10$, choosing $\Delta t = h$. For these parameters and time step scaling, the

IMEX method was shown to be unstable (Figure 5.2), but the partitioned method is stable and asymptotically approaches the theoretical convergence rate $O(\Delta t)$. The convergence rate does not approach $O(\Delta t)$ as rapidly as when κ is smaller. Table 5.6 lists the corresponding results using the partitioned method with $\kappa = 100$, and while the convergence rates have degraded in this case compared to $\kappa \le 10$, there is evidence that the convergence rate may be asymptotically approaching $O(\Delta t)$.

h	$\|\mathbf{u}(t_n) - \mathbf{u}_{part}^n\|$	rate	$\|u_1(t_n) - u_{1,part}^n\|$	rate	$\|u_2(t_n) - u_{2,part}^n\|$	rate
1/2	0.262699		0.146067		0.218078	
1/4	0.173203	0.601	0.108455	0.433	0.135043	0.691
1/8	0.106726	0.699	0.0691402	0.650	0.0813029	0.732
1/16	0.061409	0.797	0.0404435	0.774	0.0462102	0.815
1/32	0.0330993	0.892	0.0219521	0.882	0.0247723	0.899
1/64	0.0171554	0.948	0.0114099	0.944	0.012811	0.951

TABLE 5.5

Partitioned method convergence results for $\kappa = 10.0$, $\Delta t = h$

h	$\|\mathbf{u}(t_n) - \mathbf{u}_{part}^n\|$	rate	$\|u_1(t_n) - u_{1,part}^n\|$	rate	$\|u_2(t_n) - u_{2,part}^n\|$	rate
1/2	0.306537		0.195865		0.235801	
1/4	0.237524	0.368	0.161744	0.276	0.173944	0.439
1/8	0.190785	0.316	0.132736	0.285	0.137041	0.344
1/16	0.159422	0.259	0.112014	0.245	0.113438	0.273
1/32	0.128235	0.314	0.0904377	0.309	0.0909134	0.319
1/64	0.0926935	0.468	0.0654566	0.466	0.0656318	0.470

TABLE 5.6

Partitioned method convergence results for $\kappa = 100.0$, $\Delta t = h$

5.3. Second Order Numerical Schemes. The problem can also be discretized using the Crank-Nicolson method, a second order fully implicit method.

ALGORITHM 5.1 (Second-order Implicit Scheme). *Let $\Delta t > 0$, $\mathbf{f} \in L^2(\Omega)$. For each $M \in \mathbb{N}$, $M \le \frac{T}{\Delta t}$, given $\mathbf{u}^k \in X_h$, $k = 0, 1, 2, \cdots, M - 1$, find $\mathbf{u}^{k+1} \in X_h$ satisfying*

$$\frac{\mathbf{u}^{k+1} - \mathbf{u}^k}{\Delta t} + A_h \left(\frac{\mathbf{u}^{k+1} + \mathbf{u}^k}{2} \right) + B_h \left(\frac{\mathbf{u}^{k+1} + \mathbf{u}^k}{2} \right) = \mathbf{f}(t^{k+1/2}).$$

Second and higher order IMEX schemes are well known, [3], and a commonly employed example is given by Algorithm 5.2, where the operator A is discretized using Crank-Nicolson, and the interface operator B is discretized using second order Adams-Bashforth-2. Thus the algorithm is dubbed CNAB2 (ref. [3]), and provides a second order decoupled algorithm with which computations were attempted for the example problem in Section 5.1. Using the parameters $a = \nu_1 = \nu_2 = 1$ and $T = 1$ with $\kappa = 0.1$ the second order scheme achieved order $O(\Delta t^2)$ accuracy using a finite element space consisting of continuous piece-wise polynomials of degree 2, shown in Table 5.7. However, for larger values of κ no convergence was observed using CNAB2 for a reasonable time step size.

ALGORITHM 5.2 (Second-order IMEX Scheme). *Let $\Delta t > 0$, $f \in L^2(\Omega)$ and $M \le \frac{T}{\Delta t}$. Given $\mathbf{u}^k \in X_h$, $k = 0, 1, 2, \cdots, M - 1$, find $\mathbf{u}^{k+1} \in X_h$ for $M = 1, 2, \cdots, \frac{T}{\Delta t}$ satisfying*

$$\frac{\mathbf{u}^{k+1} - \mathbf{u}^k}{\Delta t} + A_h \left(\frac{\mathbf{u}^{k+1} + \mathbf{u}^k}{2} \right) + B_h \left(\frac{3}{2}\mathbf{u}^k - \frac{1}{2}\mathbf{u}^{k-1} \right) = \mathbf{f}(t^{k+1/2}).$$

Stability results for the second order IMEX algorithm are not available, except for the case A and B commute, i.e. are simultaneously diagonalizable, and some stability analysis can be performed as detailed in Section 2.1. Preliminary computational evidence suggests a general theory will not show such a stability result for CNAB2 unless possibly under a restriction on the spatial discretization. Thus a need still exists for development of efficient higher order algorithms. One possibility is to try other second-order methods as presented by Ascher, Ruuth and Wetton [3]. Second-order consistency

19

h	Δt	$\|\mathbf{u}(t_n) - \mathbf{u}_{imex}^n\|$	rate	$\|u_1(t_n) - u_{1,imex}^n\|$	rate	$\|u_2(t_n) - u_{2,imex}^n\|$	rate
1/2	1/2	0.167932		0.018283		0.166934	
1/4	1/4	0.068184	1.300	0.005730	1.674	0.067943	1.297
1/8	1/8	0.021351	1.675	0.001669	1.780	0.021286	1.674
1/16	1/16	0.005942	1.845	0.000451	1.886	0.005924	1.845
1/32	1/32	0.001565	1.925	0.000117	1.944	0.001561	1.925

TABLE 5.7

Convergence results for second order IMEX

is expected for CNAB2, so employing the technique of Burman and Fernández [8] to the CNAB2 algorithm may be sufficient, i.e. a penalty term on the boundary followed by defect correction steps to recover consistency. Furthermore, such techniques may extend directly to the fully nonlinear fluid-fluid problem, since recovery of accuracy for both spatial and time discretization errors has been proved by Labovschii [15, 16] for second-order algorithms when solving the full incompressible NSE. These are important open questions for further work.

REFERENCES

[1] R.A. Adams and J.J.F. Fournier, *Sobolev Spaces*, vol. 140 of Pure and Applied Mathematics, Academic Press, 2003.
[2] M. Anitescu, W. Layton and F. Pahlevani, Implicit for local effects and explicit for nonlocal is unconditionally stable, ETNA 18, 2004, 174-187.
[3] U. M. Ascher, S. J. Ruuth and B. T. R. Wetton, Implicit-explicit methods for time-dependent partial differential equations, SIAM J. Num. Anal. 32(3), 1995.
[4] C. Bernardi, T. Chacon-Rebello M. Gomez, R. Lewandowski, F. Murat, A model of two coupled turbulent fluids, Part II: Numerical approximations by spectral discretization, SIAM Jour. Num. Analysis, Vol. 40, No. 6, pp. 2368-2394, 2002.
[5] H. Blum, S. Lisky and R. Rannacher, A Domain Splitting Algorithm for Parabolic Problems, Computing 49, 11-23, 1992.
[6] S.C. Brenner and L.R. Scott, *The Mathematical Theory of Finite Element Methods*, Springer-Verlag, 2002.
[7] D. Bresch and J. Koko, Operator-Splitting and Lagrange Multiplier Domain Decomposition Methods for Numerical Simulation of Two Coupled Navier-Stokes Fluids, Int. J. Appl. Math. Comput. Sci., Vol. 16, No. 4, 2006, pp. 419-429.
[8] E. Burman, Miguel A. Fernández, Stabilization of explicit coupling in fluid-structure interaction involving fluid incompressibility, INRIA Research Rept. RR-6455, Feb. 2008.
[9] E. Burman, P. Hansbo, Interior penalty stabilized Lagrange multiplier for the finite element solution of elliptic interface problems, to appear in IMA Journal of Numerical Analysis. 2007
[10] P. Causin, J.-F. Gerbeau and F. Nobile, Added-mass effect in the design of partitioned algorithms for fluid-structure problems, INRIA Rept. 5084, 2004.
[11] C. N. Dawson and Q. Du, A Finite Element Domain Decomposition Method for Parabolic Equations, Fourth International Symposium on Domain Decomposition Methods for PDEs, edited by R. Glowinski et al, pp255-263, SIAM, Philadelphia, 1991.
[12] F. Hecht, A. LeHyaric and O. Pironneau. Freefem++ version 2.24-1, 2008. http://www.freefem.org/ff++.
[13] J. G. Heywood and R. Rannacher, Finite-elements approximation of the nonstationary Navier-Stokes problem part IV: Error analysis for second-order discretization. SIAM J. Numer. Anal. 1990, vol. 27(2), pp. 353-384.
[14] H. Johnston and J.-G. Liu, Accurate, stable and efficient Navier-Stokes solvers based on explicit treatment of the pressure term, J. Comput. Phys. 199 (2004), 221–259.
[15] A. Labovschii, A Defect Correction Method for the Evolutionary Convection Diffusion Problem with Increased Time Accuracy, submitted to Computational Methods in Applied Mathematics, 2007.
[16] A. Labovschii, A Defect Correction Method for the Time-Dependent Navier-Stokes Equations, (to appear in Numerical Methods for Partial Differential Equations) 2007.
[17] R. Lewandowski, *Analyse Mathématique et Océanographic*, collection RMA, Masson, 1997.
[18] W. J. Layton, *Introduction to the Numerical Analysis of Incompressible, Viscous Flows*, SIAM Comp. Sci. and Engr. 6, 2008.
[19] A. Quarteroni and A. Valli, *Numerical Approximation of Partial Differential Equations*. Springer, 1994.